

**Modification of Thin Film Composite (TFC) Membrane by Incorporation with  
Copper Nanoparticles (Cu-NPs) for Antibacterial Properties**

---

A Thesis presented to

The Faculty of the Graduate School

At the University of Missouri-Columbia

---

In Partial Fulfillment

Of the Requirements for the Degree

Master of Science

---

By

Chen Zhong

Dr. Baolin Deng, Thesis Supervisor

**July, 2014**

The undersigned, appointed by the dean of the Graduate School, have examined the thesis entitled

**Modification of Thin Film Composite (TFC) Membrane by Incorporation with  
Copper Nanoparticles (Cu-NPs) for Antibacterial Properties**

Presented by

Chen Zhong

A candidate for the degree of Master of Science in Chemical Engineering,

And hereby certify that, in their opinion, it is worthy of acceptance.

---

Professor Baolin Deng

---

Professor Paul Chan

---

Professor David G Retzloff

---

Professor Hao Li

## ACKNOWLEDGEMENTS

First and foremost, I would like to express my sincere gratitude to my advisor, Professor Baolin Deng for granting me the opportunity to work on this research project. With his support, encouragement, and guidance, the study work becomes meaningful and enjoyable.

I would also like to thank my committee members, Dr. Paul Chan, Dr. David G Retzloff and Dr. Hao Li. Dr. Chan has been my undergraduate advisor who is patient and gave me a lot of encouragement and guidance especially during my first two years. Dr. Li is a great and respectable professor in mechanical engineering with strong backgrounds of composite materials and nanotechnology. Dr. Retzloff is a knowledgeable professor in the chemical engineering department, and I want to thank him for giving me some explanations and insights into kinetics and thermodynamics during my graduate study.

My deep appreciation goes to Mr. Yin, a PhD student in our membrane group, for his patience, technical support and dedication in my research. I would like to thank Mr. Zhang who taught me how to incubate the bacteria and helped prepare some cell culture. Moreover, I want to thank all the colleagues working in Dr. Deng's research group, for their help, share, encouragement and love.

And lastly I would like to thank my parents, Mr. and Mrs. Zhong, and my dear friends for all of their encouragement and support throughout the years.

# TABLE OF CONTENTS

<b>ACKNOWLEDGEMENTS .....</b>	<b>ii</b>
<b>LIST OF TABLES .....</b>	<b>vi</b>
<b>LIST OF FIGURES .....</b>	<b>vii</b>
<b>LIST OF ABBREVIATIONS .....</b>	<b>ix</b>
<b>ABSTRACT.....</b>	<b>xi</b>
<b>CHAPTER ONE .....</b>	<b>1</b>
<b>INTRODUCTION .....</b>	<b>1</b>
1.1 The Significance of innovation in reverse osmosis membrane process.....	1
1.2 Thin film composite (TFC) membrane .....	3
1.3 Characteristics and application of TFC membrane.....	5
1.3.1 Characteristics of TFC membrane .....	5
1.3.2 Application of reverse osmosis membrane .....	8
1.4 Introduction of Copper nanoparticles (Cu-NPs) .....	9
1.4.1 Introduction of nanoparticles .....	9
1.4.2 Synthesis of copper nanoparticles.....	10
1.5 Recent research work on membrane technology with nanoparticles .....	11
1.5.1 Synthesis, immobilization and performances of Ag nanoparticles .....	13
1.5.2 Synthesis and immobilization of Cu nanoparticles.....	16
1.6 Research Objectives.....	19
<b>CHAPTER TWO .....</b>	<b>20</b>
<b>METHODOLOGY .....</b>	<b>20</b>
2.1 Synthetic methods of Polyamide/ polysulfone TFC membrane .....	20
2.1.1 Material and chemicals .....	20
2.1.2 Phase inversion process .....	21
2.1.3 In-situ interfacial polymerization process.....	21
2.2 Synthesis of Cu-NPs .....	22

2.2.1 Material and chemicals .....	22
2.2.2 Reaction with sodium borohydride as a reducing agent .....	23
2.2.3 Dialysis process .....	23
2.3 Attachment of the Cu-NPs to the TFC membranes .....	24
2.3.1 Electrostatic method.....	24
2.3.2 Covalent chemical bonding.....	24
2.4 Characterization of the Cu-NPs .....	25
2.4.1 Transmission electron microscopy (TEM).....	25
2.4.2 Zeta potential analysis.....	25
2.5 Modified TFC membranes characterization.....	26
2.5.1 Water contact angle.....	26
2.5.2 Scanning electron microscopy (SEM) .....	26
2.5.3 Attenuated total reflectance Fourier transform infrared spectroscopy (ATR-FTIR) .....	27
2.5.4 Reverse osmosis process.....	27
2.5.5 Anti-bacterial assessment.....	29
<b>CHAPTER THREE.....</b>	<b>32</b>
<b>RESULTS AND DISCUSSION .....</b>	<b>32</b>
3.1 Cu-NPs synthesis and characteristics.....	32
3.1.1 Synthesis of Cu-NPs .....	32
3.1.2 Mean diameters of the Cu-NPs .....	35
3.1.3 Zeta potential of Cu-NPs.....	37
3.2 Membrane properties .....	38
3.2.1 Contact angles.....	38
3.2.2 SEM images of membranes loaded with Cu-NPs .....	40
3.2.3 ATR-FTIR spectra analysis .....	46
3.3 Membrane Performance for Desalination .....	47
3.3.1 Pure water test.....	47
3.3.2 Desalination process .....	48
3.4 Antibacterial properties of the membrane surface .....	49
3.4.1 Disk Tests.....	49
3.4.2 SEM investigation.....	53

<b>CHAPTER FOUR.....</b>	<b>55</b>
<b>CONCLUSIONS AND FUTURE STUDIES .....</b>	<b>55</b>
4.1 Conclusions.....	55
4.2 Future studies .....	56
<b>BIBLIOGRAPHY .....</b>	<b>57</b>

## **LIST OF TABLES**

Table 1.1 Classification of the particles according to diameter range ..... 9

## LIST OF FIGURES

Fig 1.1 Conceptual illustration of (a) TFC and (b) TFN membrane structures (Jeong, Hoek et al. 2007) .....	2
Fig 1.2 Illustration of Membrane separation process.....	3
Fig 2.1 The schematic diagram of reverse osmosis filtration system .....	27
Fig 3.1 Cu-NPs preparation procedure with color changes .....	33
Fig 3.2 TEM image of Cu-NPs suspension solution with the scale of 100nm and 50nm .....	35
Fig 3.3 Distribution of Cu-NPs of different diameters (nm) .....	36
Fig 3.4 Zeta potential of Cu-NPs at different PH values (5.0-11.2) .....	37
Fig 3.5 Water contact angle of different membrane surfaces .....	38
Fig 3.6 SEM image of the membrane after immersing in the cysteamine/ethanol solution for 24hrs.....	40
Fig 3.7 SEM surface morphology of Cu-NPs incorporated TFC membrane. (a) is fabricated via electrostatic method TFC-CuNPs; (b) is made via covalent bonding TFC-S-CuNPs.....	41
Fig 3.8 Bigger magnifications with detailed the structure of the membrane surface: (a) TFC (b) TFC-CuNPs (c) TFC-S-CuNPs.....	43
Fig 3.9 EDS test to analysis the elements existed on the surface of the Cu-NPs incorporated membranes .....	44
Fig 3.10 SEM images of the (a) TFC-CuNPs (b) TFC-S-CuNPs membranes after the desalination test.....	45
Fig 3.11 ATR-FTIR spectra analysis of the membrane surface .....	46
Fig 3.12 Pure water flux of membrane samples .....	47
Fig 3.13 Salt rejection and water flux of membrane samples.....	48
Fig 3.14 Disk test with <i>P. aeruginosa</i> incubation (a) Plain LB disk; (b) TFC surface in contact with the bacteria cell culture before peeling off; (c) colony contacted with TFC; (d) TFC surface; (e) colony contacted with TFC-CuNPs; (f)TFC-CuNPs surface; (g) colony contacted with TFC-S-CuNPs; (h) TFC-S-CuNPs surface.....	51

Fig 3.15 Disk test of *P. aeruginosa* incubation with the left side covered with TFC-CuNPs, the right side covered with TFC-S-CuNPs; The Cu-NPs on both membranes had been released for 7 days ..... 52

Fig 3.16 SEM images of membrane surfaces shacked with *P. aeruginosa*-PBS suspension solution for 6h and fixed by GA solution for 5h. (a) TFC (b) alive *P. aeruginosa* (c) TFC-Cu (d) TFC-SH-CuNPs ..... 54

## LIST OF ABBREVIATIONS

RO	Reverse osmosis
Cu-NPs	Copper nanoparticles
PSF	Polysulfone
PA	Polyamide
TFC	Thin film composite
TFN	Thin film nanocomposite
CTAB	Cetyl trimethylammonium bromide
DMF	Dimethyl formamide
IP	Interfacial polymerization
MPD	m-Phenylenediamine
TMC	Trimesoyl chloride
MSF	Multi-stage flash
MED	Multi-effect distillation
PES	Polyethersulfone
MWCO	Molecular weight cut-off
SEM	Scanning electron microscope
EDS	Energy-dispersive X-ray spectroscopy
ATF-FTIR	Attenuated total reflectance Fourier transform infrared spectroscopy
DI water	Deionized water
TEM	Transmission electron microscopy
PBS	Phosphate-buffered saline
TAP	2, 4, 6-Triaminopyrimidine

ICP-OES	Inductively coupled plasma-optical emission spectrometer
PEI	Polyethyleneimine
PAN	Polyacrylonitrile
LB	Luria Bertani
GA	Glutaraldehyde

## ABSTRACT

Membrane biofouling has been a challenging problem restricting the application of reverse osmosis (RO) desalination process. Copper is known for its antimicrobial properties and is easily available with low cost. In this paper, copper nanoparticles (Cu-NPs) with a mean diameter of 15nm were synthesized by the reduction of copper (II) chloride with sodium borohydride ( $\text{NaBH}_4$ ), using cetyl trimethylammonium bromide ( $(\text{C}_{16}\text{H}_{33})\text{N}(\text{CH}_3)_3\text{Br}$ , CTAB) as a capping agent. After purification of Cu-NPs by dialysis, the particles were successfully immobilized onto the surface of thin film composite (TFC) membranes via either electrostatic interactions or by covalent bonding with cysteamine as a linker. The electrostatic method was simply to immerse the newly made TFC membranes to the Cu-NPs suspension. Since the CTAB had formed cationic bilayer outside the Cu-NPs, the Cu-NPs was not only adsorbed on the membranes but also attached to the surface because of the electrostatic effect with the negatively charged membrane surface. The covalent bonding method utilized cysteamine ( $\text{C}_4\text{H}_{12}\text{N}_2\text{S}_2$ ) to activate the thin film layer with thiol functional groups first and then incorporated the metallic copper nanoparticles to form the stable covalent chemical bonding in between. The resulting membranes by these two methods were labeled as TFC-CuNPs and TFC-S-CuNPs, respectively, in this study. Scanning electron microscopy (SEM) imaging and associated energy-dispersive X-ray spectroscopy (EDS) showed that large amounts of Cu-NPs existed on both types of membranes. Surface hydrophilicity of the membranes was enhanced by the presence of Cu-NPs, as indicated by the measured contact angle of  $63.25 \pm 0.75$  for TFC,  $38.63 \pm 2.16$  for TFC-CuNPs, and  $58.00 \pm 3.39$  for TFC-S-CuNPs. Consistently, the water flux obtained from the RO desalination system was increased from  $47.07 \pm 0.84$  for TFC,  $49.10 \pm 0.22$  for TFC-CuNPs, and  $69.13 \pm 1.43$  for TFC-S-CuNPs, with this increase in hydrophilicity. The salt rejection based on NaCl was slightly

decreased for both modified membranes when compared with the original TFC. The TFC membranes with Cu-NPs both exhibited excellent antibacterial properties against *P. aeruginosa* based on the disk incubation test and the SEM observation. Moreover, TFC-S-CuNPs were more stable and with better anti-bacterial properties than TFC-CuNPs.

# CHAPTER ONE

## INTRODUCTION

### **1.1 The Significance of innovation in reverse osmosis membrane process**

Water scarcity has become a worldwide concern which is being recognized as a huge threat to human activities especially in water-stressed countries. Consequently, efforts have been made to develop resources such as the desalination process. Compared with traditional thermal processes such as multi-stage flash (MSF) and multi-effect distillation (MED), the reverse osmosis (RO) membrane process is advantageous due to its low cost, ease of operation and high efficiency (Fritzmann, Löwenberg et al. 2007). Nowadays, RO membrane desalination has dominated the new plant installations market after experiencing fast growth over the past 40 years. Nevertheless, while the modern RO technology has shown high performance, low cost, and industrial scale manufacturing capability, several significant challenges still remain in the RO desalination field, in particular membrane fouling (Greenlee 2009).

Membrane fouling phenomena are unavoidable and greatly constrain the efficacy of practical application. Fouling occurs when the surface is coated with contaminants, thus increasing the resistance to the driving force (Committee 2005). Under such circumstances, a higher driving force is needed, which results in an increased energy consumption. Also, the performance of membrane decreases with time. Many attempts have been made to modify membrane surfaces for higher hydrophilicity and antibacterial properties that may help control membrane fouling.

In recent years, the emergence of nanotechnology offered an entirely new world for functional materials with excellent properties. A new concept of thin film nanocomposite (TFN) has been proposed in which nanomaterials are incorporated into the thin film layer of TFC membranes via the in-situ interfacial polymerization for desalination (Fig 1.1) (Jeong, Hoek et al. 2007). Other work was also conducted on surface modification of TFC membrane to immobilize functional nanoparticles for better performances. Metallic based nanoparticles, notably silver, have attracted much attention because of their long history as biocides (Kim, Kwak et al. 2003, Lee, Kim et al. 2007, Yin, Yang et al. 2013).

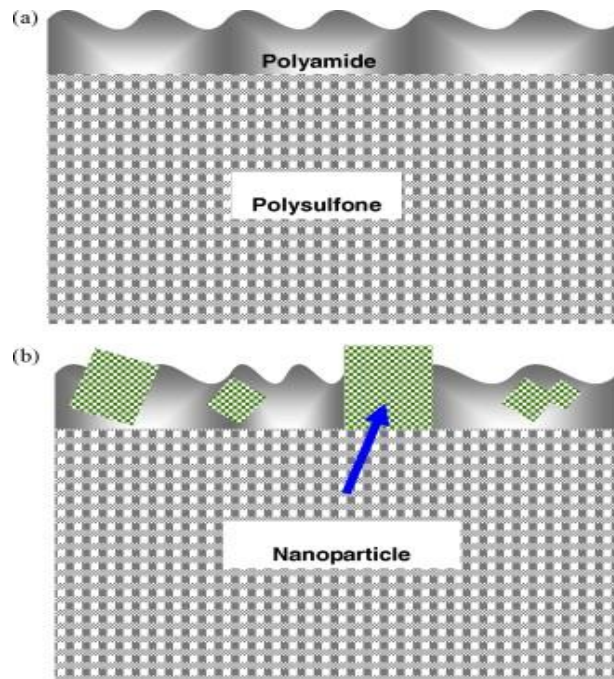


**Fig 1.1 Conceptual illustration of (a) TFC and (b) TFN membrane structures (Jeong, Hoek et al. 2007)**

Although achievements have been made to improve the current state of membrane technology, it still takes years to optimize the desalination performance and antifouling properties to meet the increasing global demands for clean water. In this study, TFC

membranes with copper nanoparticles (Cu-NPs) were fabricated and assessed for their antifouling properties. The CuNPs was synthesized first and then embedded to the TFC membrane via electrostatic interaction or covalent bonding. The antifouling characteristics and performance of the membranes were evaluated and compared.

## 1.2 Thin film composite (TFC) membrane

In general, membrane acts as a selective barrier between the feed phase and the permeate phase under a certain driving force. Depending on the types of membrane with various structures and the components, particles and/or solutes would be rejected by the membrane and remain in the feed phase or retentate phase, while other smaller constituents can pass through the barrier and go to the permeate phase. The driving force, which is usually a certain gradient between two phases such as the concentration, temperature and trans-membrane pressure, plays an important role to the separation (Beerlage 1994).

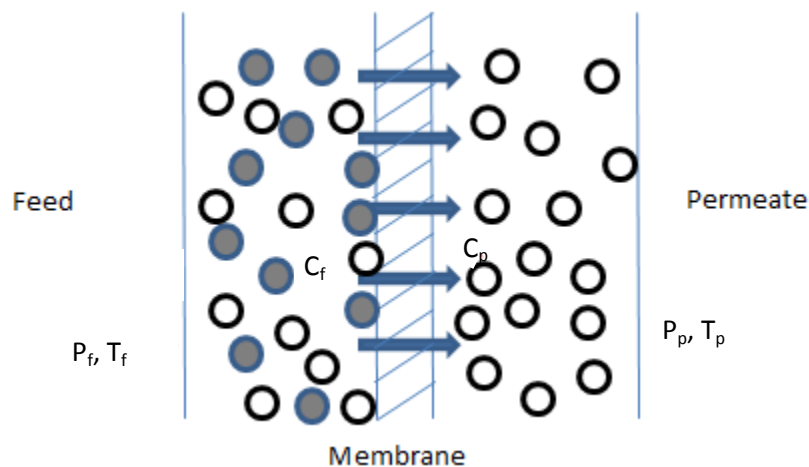


Fig 1.2 Illustration of Membrane separation process

Thin film composite (TFC) membrane is a semipermeable asymmetric membrane consisted of a microporous substrate layer and a thin functional layer. The substrate layer serves as a mechanical support, while the functional layer controls solute rejection and permeate flux. Membranes used in the reverse osmosis (RO) process are typically made of a polyamide thin film and polysulfone (PSF) or polyethersulfone (PES) substrate layer. The fabrication of TFC membrane involves two-step casting, which enables individual optimization of the materials and structures for support membrane and for the barrier layer. Polysulfone has been considered a good material for the support layer due to its good resistance to compaction, reasonable flux and its stability in a wide range of PH value. The thin film polyamide functional layer can be modified in multiple ways to obtain desired properties such as higher hydrophilicity and antimicrobial effect (Lee, Arnot et al. 2011).

For reverse osmosis (RO) where water is driven across a semipermeable membrane under pressure while salt is rejected, polyamide-polysulfone (PA/PSF) RO membrane is the most widely used membrane. Polysulfone substrate layer was formed first via the non-solvent induced phase inversion method, and then in-situ interfacial polymerization was conducted to form the functional thin film layer. Although the thin film layer has the dominant effect in the desalination performance, the structure of the substrate layer still has an impact and needs to be optimized. For example, a study on the impact of support membrane structure and content indicated that the ultrafiltration membrane made from 15wt.% of polysulfone in dimethyl formamide (DMF) was good of use as a support layer for making RO membrane.

## 1.3 Characteristics and application of TFC membrane

### 1.3.1 Characteristics of TFC membrane

In evaluating the performance of RO process, important parameters are water flux that is primarily controlled by transmembrane pressure and salt rejection that is mainly determined by solute diffusion. For an ideal TFC membrane, the water flux should be as high as possible, so the treatment process would be more efficient. Meanwhile, a relatively high rejection is preferred, which is related to the water quality of permeate. There is a trade-off between these two parameters. The equations below defined the relationships between the flux and pressure gradient and between the salt rejection and solute concentration gradient across the membrane.

$$J = A(\Delta P - \Delta\pi) \quad (1-1)$$

$J$  ---Water flux

$A$ ---Constant

$\Delta P$ ---Pressure gradient across the membrane

$\Delta\pi$ ---Osmotic pressure gradient across the membrane, which is caused due to the concentration difference between the feed and the permeates

According to the equation, if  $\Delta P < \Delta\pi$ , water in the permeate side would flow back to dilute the feed side to balance the concentration difference. If  $\Delta P = \Delta\pi$ , no flow occurs. If  $\Delta P > \Delta\pi$ , the reverse osmosis process happens, and the flux increases as the pressure differences become larger

$$R = \left(1 - \frac{C_p}{C_f}\right) \times 100\% \quad (1-2)$$

R --- Salt rejection

$C_p$ --- Salt concentration of permeate solution

$C_f$ --- Salt concentration of feed solution

During the desalination process evaluation as being conducted in this study, the feed solution is contained in a tank with big volume, so there is negligible change in the feed concentration  $C_f$ . Herby, the salt rejection is mainly calculated based on the permeate concentration  $C_p$ . Other influences that constrain flux and salt rejection could be the mechanical and chemical-resistance properties. For example, when the applied pressure is over the limit that the membrane could stand, the membrane breakage may occur. The membrane should also be chlorine-resistant, stable in a wide range of operating pH values (typically 3 – 11), resistant to compaction, and able to be operated at relatively high temperature without damage (Cadotte, Petersen et al. 1980).

In this study, various methods and instruments are utilized to characterize the physicochemical properties of the membranes. The methods are listed below:

- Determination of molecular weight cut-off (MWCO)

Molecular weight cut-off of a membrane indicates the lowest molecular weight of solute that can be retained by the membrane at normally 90% level. It is generally specified by the manufacturers but can also be determined by measuring rejection of solutes with a range of molecular weights.

- Water contact angle

The water contact angle can be used as a measure of the hydrophilicity of the membrane surface. A low contact angle indicates that the water droplet would spread easily to a hydrophilic surface material is hydrophilic, and vice versa, a high contact angle suggests the water droplet does not spread much. When the hydrophilicity of RO and nanofiltration membrane surfaces is increased, their performances for water filtration as well as antifouling properties often increase.

- Scanning electron microscope (SEM )

The morphology of the surface and cross-section of the membrane could be examined through the Scanning electron microscopy. In this study, SEM is used to observe and compare the structures of different membrane samples as well as copper nanoparticles and bacterial cells. Furthermore, the associated Energy-dispersive X-ray spectroscopy (EDS) offers the possibility to conduct the elements analysis.

- Attenuated total reflectance Fourier transform infrared spectroscopy (ATF-FTIR)

The chemical bonding that contained on the surface of the membrane could be examined through the attenuated total reflectance Fourier transform infrared spectroscopy. The peak occurring at specific wave number ( $\text{cm}^{-1}$ ) demonstrates what kind of bonding it is and how strong it acts.

### **1.3.2 Application of reverse osmosis membrane**

Reverse osmosis system is playing a critical role in water treatment, as the needs increase for water desalination, waste water reuse, and ultrapure water production. As reported by the American water works association, the advanced innovations in membrane technology has been successfully applied to some large municipal projects such as the Orange County Water District's Groundwater Replenishment System. The improved permeability, high solute rejection and enhanced anti-fouling properties have contributed significantly to the cost-effectiveness of the water treatment plants (Shu, Majamaa et al. 2014). For desalination process, according to the International desalination association, in the year of 2011, 66% of installed desalination capacity (44.5 of 67.4 Mm<sup>3</sup>/day) is based on reverse osmosis. Almost all new plants built in that year considered reverse osmosis system as their main focus.

In addition to water treatment and desalination, reverse osmosis have a big great market in some food industries. Especially for the juice, wine and dairy industries, the concentrating operation by reverse osmosis process instead of heat-treatment could save energy consumption and avoid heat-sensitive products from being exposed to the high temperatures and thereby losing flavor.

## 1.4 Introduction of Copper nanoparticles (Cu-NPs)

### 1.4.1 Introduction of nanoparticles

The emergence of nano-science and nanotechnology has led to an exponential increase in the research and publications on nanoparticles, as they could be applied to a variety of fields due to their unique self-assembling, antibacterial, magnetic and optical properties (Daniel and Astruc 2004). Particles could be categorized based on sizes as shown in Table 1.1.

**Table 1.1 Classification of the particles according to diameter range**

Diameter range	2,500~10,000 nm	100~2,500 nm	1~100 nm
Classifications	Coarse particles	Fine particles	Ultrafine particles (nanoparticles)

Metallic nanoparticles have attracted great interests in membrane fabrication and modification due to their special physical and chemical properties. The sizes and shapes of the nanoparticles could be varied according to different synthesis methods. Usually, the smaller nanoparticles are more reaction due to higher specific surface areas. For the control of microbial fouling, although silver has been the main focus in early research, recently copper has gained much attention as it is relatively low in cost and easily available (Benavente, Lozano et al. 2013). However, many challenges exist for using copper as an anti-fouling agent. For example, it can be relatively easily oxidized so its long term effectiveness needs to be assessed. Proper dispersion of copper nanoparticles in membrane preparation also needs to be addressed.

### **1.4.2 Synthesis of copper nanoparticles**

Copper nanoparticles can be synthesized through numerous techniques, such as thermal reduction, sonochemical reduction (Dhas, Raj et al. 1998), chemical reductions, nanostructured templates, and gas condensation. The preparation conditions and methods often control the particle size, shape, and other chemical and physical properties.

Among these approaches, chemical reduction methods are commonly used to synthesize copper nanoparticles. Huang. et al utilized excess amount of hydrazine to reduce copper ions to metallic nanoparticles under N<sub>2</sub> inert gas to prevent oxidation (Huang, Yan et al. 1997). Khanna et al. synthesized pure copper nanoparticles without the oxidants by reducing the copper salt by sodium citrate/SFS and myristic acid/SFS (Khanna, Gaikwad et al. 2007). Park et al conducted the aqueous chemical reduction by using diethyleneglycol not only as a reaction medium but also as a reducing agent. The electron released by diethyleneglycol could reduce copper ions to metallic nanoparticles (Park, Jeong et al. 2007).

Concerning the potential to control the morphology and structure of newly synthesized copper nanoparticles, preparation conditions such as temperature and amount of reducing agent are important. The chemical reduction of copper ions to form different shapes of copper nano-crystals was investigated using an AOT surfactant in water/isooctane system. The shape was found to depend on the concentration of reducing agents (Salzemann, Lisiecki et al. 2004). Based on this result, Mott, D designed a series of experiments to form size-controllable and potentially shape-controllable copper nanoparticles by manipulating the reaction temperature and the amount of the reducing agents (Mott, Galkowski et al. 2007).

## **1.5 Recent research work on membrane technology with nanoparticles**

Biofouling phenomenon and its control have limited the application of membrane separation processes in many fields, such as membrane bioreactor and water treatment. The biofouling is undesired because it decreases the permeate flux and may lower the quality of permeate. Thus a lot of work has been done to control biofouling in order to maintain the high performance of the membrane system. Pre-treatments are widely used to partly prevent the biofouling. In order to recover performance loss caused by the biofouling in the operations, cleaning procedures are also taken to reduce the degree of fouling. Despite the high cost of such procedures and maintenances, membranes still need to be replaced after a period of usage if the extent of biofouling is severe or if some degradation of membrane occurs because of those physical and chemical treatments.

One way to solve this challenging issue is to modify the membrane itself to be antifouling and thus prevent the forming of bio-film on the surfaces and extend the service life of the membranes. Various functional groups and biocidal agents have been introduced to improve the membrane hydrophilicity and antibacterial property in order to reduce the biofouling. The modified surface with higher hydrophilicity may prevent the adhesion and deposition of those microorganisms effectively. However, to reduce the biofilm formed by the bacteria, biocides agents are more effective and thus preferred.

There has been a great deal of research focusing on immobilization of biocides onto the membrane surface, such as phenols, quaternary ammonium salts and metal ions. Among the metal biocides, some nanoparticles such as silver (Ag), copper (Cu), zinc oxide (ZnO) and titanium oxide (TiO<sub>2</sub>) showed high toxicity to a lot of microorganisms including bacteria, fungi and viruses. Silver is a widely studied anti-bacterial agent in many

application fields. Ag nanoparticles have large surface-to-volume ratio and can serve sustainably as biocides. Chamakura et al. described in detail the antibacterial mechanism of Ag-NPs, focusing mainly on the interaction between the nanoparticles and the targets and the generation of the reactive oxygen species (ROS) (Chamakura, Perez-Ballesteros et al. 2011). For membrane preparation, some blended the Ag-NPs directly in the dope polymer solution during the phase inversion process. Others coated the Ag-NPs on the surface to increase the hydrophilicity and anti-fouling property (Basri, Ismail et al. 2010, Cao, Tang et al. 2010, Zhu, Bai et al. 2010, Sawada, Fachrul et al. 2012, Koseoglu-Imer, Kose et al. 2013, Yin, Yang et al. 2013).

Compared to silver, copper is a promising candidate in membrane modification since it is cheaper and less cytotoxic to human. Copper nanoparticles also have excellent antibacterial properties since it can release some  $\text{Cu}^{2+}$  ions and work as biocides. Some researchers dipped the membrane with the copper ions solution to adsorb  $\text{Cu}^{2+}$  ions and reach the goal of improved antifouling properties. In the long term, however, copper nanoparticles would work better because they could produce  $\text{Cu}^{2+}$  ions for a significant time period.

This section reviewed the research works on improving the membrane anti-fouling property by immobilization of metal ions, mainly about silver and copper nanoparticles. The synthesis methods and approaches, and the performances of the modified membrane are illustrated and compared. Through the review process, we gain a better insight into this field and some inspirations for further studies.

### 1.5.1 Synthesis, immobilization and performances of Ag nanoparticles

#### 1. Phase inversion method with biocides in the dope solution

Derya et al. synthesized the polysulfone (PSF) membranes by adding different amounts of silver nanoparticles Ag-NPs (0-1 wt. %) into the dope solution. The results suggested that 1.0 AgNP-PS composite membrane showed the best protein filtration performance while 0.25AgNP-PS composite membrane had the best carbohydrate filtration performance. In the active sludge filtration process, 0.25AgNP-PS composite membrane had the highest permeate volume, while the bare PS membrane had the lowest. That's because the fouling phenomenon is proportional to the roughness of the surface of the membrane. The growth of the bacterial colonies decreased with increasing Ag-NPs ratio, which demonstrated the improved antibacterial performance of PS membranes (Koseoglu-Imer, Kose et al. 2013).

Similarly, H. Basri et al. added  $\text{AgNO}_3$  directly to the dope PES solution with addition of dispersant to prepare the ultrafiltration membrane via the phase inversion method. They compared two different dispersants, PVP and 2, 4, 6-triaminopyrimidin (TAP) in the case of effects on the PES-Ag membrane, and found that the additive could reduce the silver leaching. The anti-bacterial performance of the modified membrane was evidenced by larger inhibit ring formed in the agar diffusion test. In the anti-fouling test, the PES-TAP- $\text{AgNO}_3$  appeared to inhibit almost 100% bacterial growth in rich medium. In another paper, Basri et al compared the different membranes with PVP of different molecular weight 10,000, 40,000 and 360,000 Da as dispersant. The result indicated that the PES membrane with 360,000 Da exhibited a higher concentration of Ag and uniform

distribution, which ensures 100% inhibition of *E. coli* growth within 24 h incubation (Basri, Ismail et al. 2010).

## 2. Ag-NPs membrane modified with reducing agents or functional groups

Zhu et al. successfully immobilized ionic or reduced silver onto the surface of a chitosan (CS) membrane and the anti-biofouling performance were found to be effective (Zhu, Bai et al. 2010). In their preparation process, silver ions were first immobilized onto the membranes and then reduced by reducing agent. A chitosan membrane was immersed into 0.05M  $\text{AgNO}_3$  solution to immobilize silver ions onto the surface, denoted as CS\_Ag<sup>+</sup>. After being washed and dried, the membrane was oxidized by a 0.01 M ascorbic acid solution for 1 min, turning silver ions to metallic silver, which is denoted as CS\_Ag<sup>0</sup>. During the immobilization process, the concentrations of the metal ions are analyzed with an inductively coupled plasma-optical emission spectrometer (ICP-OES). It shows that the amounts of CS\_Ag<sup>+</sup> and CS\_Ag<sup>0</sup> were approximately 51mg and 47.4mg, respectively. After the leaching, 27% of Ag ions were leached out, while less than 1% reduced silver was leached. The possible reason was that the reduced silver was more difficult to be dissolved or ion-exchanged. The disk diffusion experiments showed that both *E. coli* and *pseudomonas sp.* were unable to grow on the CS\_Ag<sup>+</sup> and CS\_Ag<sup>0</sup> membranes. Moreover, the modified membrane show overall good anti-biofouling performance at a high bacterial concentration. These results demonstrated that the immobilization of silver onto membrane surface can be effective to improve the anti-biofouling property (Zhu, Bai et al. 2010).

Cao et al. first introduced the Ag-NPs onto the sulfonated polyethersulfone SPES/PES membrane by using Vitamin C (ascorbic acid) as the reducing agent (Cao, Tang et al. 2010). The hybrid membranes with a weight ratio of PES/SPES=3/2 were immersed in AgNO<sub>3</sub> solution, followed by silver ion reduction in the ascorbic acid solution to silver nanoparticles with diameters around 40-50nm. These nanoparticles caused bacteriostatic and bactericidal impact on the membrane for a long duration. Additionally, the cytotoxicity level was tested to be within the safety range (Cao, Tang et al. 2010).

Sawada et al. examined both organic antifouling and antibacterial properties by grafting acrylamide onto a PES membrane and then introducing the Ag-NPs in the acrylamide layer (Sawada, Fachrul et al. 2012). The hydrophilicity of the membrane was found to increase so that the fouling caused by the BSA was reduced. Moreover, the membrane containing the Ag-NPs can inhibit growth of *E. coli* effectively and thus has a strong anti-biofouling property (Sawada, Fachrul et al. 2012).

Yin et al. attached silver nanoparticles (Ag-NPs) onto thin-film (TFC) membranes through covalent bonding to reduce membrane fouling. Ag-NPs, with around 15nm in diameter, was first used as a reducing agent to oxidize the Ag<sup>+</sup> in the AgNO<sub>3</sub> /PVP40 water solution. Then Ag-NPs were effectively attached onto the surface of polyamide (PA) TFC membrane by using cysteamine as a bridging agent. The water flux was increased by the modification from 49.8 to 69.4 L/m<sup>2</sup>h, while there's a slight decrease in the salt rejection from 95.5% to 93.6%. It is suggested that the ethanol used in the grafting process could lead to membrane swelling and cause a looser structure of the membrane. The leaching of silver nanoparticles was minimal and the functionalized

membrane exhibited improved anti-bacterial property that could inhibit the growth of *E. coli* (Yin, Yang et al. 2013).

### **1.5.2 Synthesis and immobilization of Cu nanoparticles**

Copper is another metals that has been often explored for its antibacterial properties. Here we briefly summarize the synthesis and immobilization of copper nanoparticles for membrane applications.

#### **1. Physical deposition and adsorption**

Isloor et al. studied the copper coated polysulfone/ modified poly isobutylene alt-maleic anhydride blend membrane and its anti-biofouling property (Isloor, Ganesh et al. 2013). The deposition of copper was performed by physical vapor method, which means evaporating the copper in a tungsten basket. The thickness of Cu coating was controlled by the deposition time. The membrane showed 96% salt rejection and 36L/m<sup>2</sup>h water flux. Also, the coated membrane has good inhibition against *B. cereus* bacterial growth and excellent anti-biofouling property (Isloor, Ganesh et al. 2013).

Zhu et al. prepared heparinized copper hydroxide nanofibers membrane by filtration and deposition of the heparinized Cu(OH)<sub>2</sub> nano-fibers onto a PSF membrane (Zhu, Zhu et al. 2013). These nano-fibers were made by the electrostatic interaction between the positively charged Cu(OH)<sub>2</sub> and negatively charged heparin, whereas the Cu(OH)<sub>2</sub> nano-fibers were prepared in a weakly alkaline copper nitrate solution in the presence of 2-aminoethanol (Zhu, Zhu et al. 2013).

Karkhanechi et al. immersed the commercial RO membrane into the copper hydroxide ( $\text{Cu}(\text{OH})_2$ ) nanoparticles suspension solution for adsorption process. The modified membrane showed good antibacterial property, which was attributed to the release of  $\text{Cu}^{2+}$  ions from the particles (Karkhanechi, Takagi et al. 2013).

## 2. Phase inversion method with biocides in the dope solution

Akar et al. casted PES ultrafiltration membranes with selenium nanoparticles and copper nanoparticles by phase inversion process. The nano-scale particles of metallic copper were synthesized by sono-chemical reduction of copper (II) hydrazine carboxylate  $\text{Cu}(\text{N}_2\text{H}_3\text{COO})_2 \cdot 2\text{H}_2\text{O}$  complex in an aqueous medium under an argon atmosphere (Akar, Asar et al. 2013).

Dang et al. added  $\text{CuCl}_2$  and PVP as additives to the PES dope solution to produce the three-bore PES hollow fiber UF membrane with antibacterial properties by phase inversion method (Dang, Zhang et al. 2012).

Chen et al. added halloysite nanotubes loaded with copper ions ( $\text{Cu}^{2+}$ -HNTs) as an antibacterial agent to the PES dope solution to prepare the UF membrane by the phase inversion method. The  $\text{Cu}^{2+}$ -HNTs were synthesized by chemical modification of HNTs with silane coupling agent and then mixed with copper dichloride for complexing copper ions (Chen, Zhang et al. 2012).

## 3. Membrane surface modified with functional groups and immobilization of copper ions

Qiu et al. utilized surface-initiated atom transfer radical polymerization (SI-ATRP) to graft the poly (4-vinylpyridine) (P4VP) brushes on to the PSF membrane surface and then immobilized copper (II) ions to the surface (Qiu, Zhang et al. 2011).

Xu et al. developed an antibacterial UF membrane by depositing polyethyleneimine (PEI) onto a microporous polyacrylonitrile (PAN) membrane surface via the electrostatic self-assembly followed by immobilization of copper (II) ions on the surface. It can serve as an effective biocide for a long time in the seawater desalination (Xu, Feng et al. 2012).

Ben-Sasson et al. synthesized positively charged Cu-NPs using polyethyleneimine (PEI) as capping agent. This allowed the simple electrostatic functionalization of the negatively charged membrane surface. The functionalization exhibited significant antimicrobial properties, leading to an 80-95% reduction in the number of attached live bacteria (Benavente, Lozano et al. 2013).

## 1.6 Research Objectives

The anti-bacterial properties of the Ag-NPs and Cu-NPs have the potential to be explored for making better filtration membranes. Ag-NPs, in particular, has a long history as biocides and been intensively studied. Copper, in contrast, has been less studied even though it is cheaper, easily available and less cytotoxic, partially because of the concern on its long term effectiveness. It is therefore important to investigate the method of immobilizing CuNPs so its long-term effectiveness can be maintained for anti biofouling applications.

The objectives of this study were to synthesize Cu-NPs with appropriate diameter, prepare RO/nanofiltration membranes containing these particles, and evaluate the performance and anti-bacterial characteristics of the membranes. Cu-NPs will be synthesized by sodium borohydride ( $\text{NaBH}_4$ ) reduction in the aqueous phase, with cetyl trimethylammonium bromide ( $((\text{C}_{16}\text{H}_{33})\text{N}(\text{CH}_3)_3\text{Br}$ , CTAB) as a capping agent. The newly synthesized nanoparticles were positively charged, which enables electrostatic bonding with negatively charged membrane surface. Another approach is to use the covalent bonding for the attachment of CuNPs by functionalizing the surface with cysteamine. The thin film composite (TFC) membranes with or without CuNPs will be assessed and compared in terms of their performance (water flux and salt rejection) and antibacterial characteristics.

## CHAPTER TWO

### METHODOLOGY

#### 2.1 Synthetic methods of Polyamide/ polysulfone TFC membrane

##### 2.1.1 Material and chemicals

Polysulfone (PSF) is widely used to prepare the dope solution for substrate membrane. Its excellent mechanical properties, relatively low cost and availability make it a competitive polymer in the membrane field. In this research, PSF was purchased from Sigma-Aldrich, with an average molecular weight of 35,000 Da.

N-N-Dimethyl formamide (DMF) was selected as the organic solvent for polysulfone beads. Anhydrous DMF (99.8%) was also purchased from Sigma-Aldrich.

1, 3- Phenylenediamine (MPD, powder, >99.8%) and 1, 3, 5-benzenetricarbonyl trimesoyl chloride (TMC, 98%), both from Sigma-Aldrich, were used for the interfacial polymerization (IP) to prepare for the polyamide functional thin film on the surface of polysulfone substrate layer.

Hexane (>95%), from Sigma-Aldrich, was used as the solvent for TMC and also the agent to wash the membrane surface after IP in order to remove the excess chemicals.

Deionized (DI) water, obtained from a Milli-Q ultrapure water purification system (Synergy 185, 18.2 M $\Omega$ ·cm, EMD Millipore Corp., Billerica, MA) was used for the solution preparation and reverse osmosis filtration process.

All chemicals were of ACS reagent grades and used without further purification.

### **2.1.2 Phase inversion process**

To prepare the casting dope solution, 15wt% PSF beads and 85wt% DMF solution were added to an airtight bottle and stirred at 50°C for 6 h. After the PSF were completely dissolved in the DMF solution, the dope solution was kept overnight for degassing at room temperature.

The flat sheet PSF support layer was fabricated by the phase inversion method. The dope solution was spread on a clean glass via a casting knife (EQ-Se-KTQ-150, MTI Corp., Richmond, CA) at the thickness adjusted to approximately 100  $\mu\text{m}$ . The glass and the entire assembly were immediately immersed into a DI water bath (25°C). The PSF membrane precipitated once contacted with water and the color of the membrane converted from transparent to white. The PSF membrane gradually separated itself from the glass plate and was removed from the water bath after 10 min. Each membrane was thoroughly washed and stored in DI water for at least 24 h before use.

### **2.1.3 In-situ interfacial polymerization process**

The In-situ interfacial polymerization was conducted to form the functional thin layer on top of the supporting PSF membrane. To begin with, the PSF membrane was attached onto a small glass plate and washed thoroughly with DI water. Excess water from the membrane was removed via a rubber roller. About 2-3 ml 2.0wt% MPD-DI water solution was spread on the most area of membrane surface. After 3 min, excess MPD was removed by a rubber roller and the surface was soaked in a 0.15wt% TMC-hexane solution for 30s. This procedure enabled the polymerization reaction to form a dense polyamide (PA) thin layer on the top the substrate layer. The TFC membrane was then

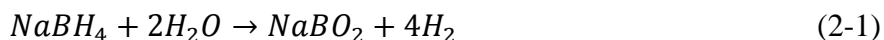
rinsed with pure hexane to remove the excess reacting solution. Finally, the newly made TFC membrane was dried at 80°C for 5 min and stored in DI water at 4 °C before use.

## 2.2 Synthesis of Cu-NPs

### 2.2.1 Material and chemicals

Copper Chloride ( $\text{CuCl}_2$ ), sodium borohydride powder ( $\text{NaBH}_4$ , >98%), ammonia solution (28.0-30.0%  $\text{NH}_3$  basis), Cetyl trimethylammonium bromide ( $(\text{C}_{16}\text{H}_{33})\text{N}(\text{CH}_3)_3\text{Br}$ , CTAB), were all purchased from Sigma-Aldrich. The chemicals were all of ACS reagent grades and used without further purification.

Copper chloride is the salt containing the copper ions, which could be reduced to metallic Cu-NPs by the sodium borohydride. In this project, sodium borohydride served as a hydrogen source that reduced the copper (II) chloride to the metallic copper.



CTAB was used as the capping agent in the reaction to prevent agglomeration of the metallic Cu-NPs. As a cationic surfactant capable of forming a bi-layer on the surface of the Cu-NPs, it was positively charged and could be attached to the negatively-charged membrane surface through electrostatic forces. Moreover, it was an antiseptic cetrimide effective against bacteria and fungi. Thus, to some extent, the bi-layer of CTAB could enhance the antibacterial property of the copper nanoparticles and subsequently the the nanocomposite membranes with CuNPs.

### **2.2.2 Reaction with sodium borohydride as a reducing agent**

The metallic Cu-NPs suspension solution was achieved by the reduction reaction, which typically was carried out in a capped bottle by mixing equal volumes of two aqueous CTAB solutions (10mM): one contained 50ml copper chloride (50mM) with the pH value adjusted to 10 using ammonia solution, and the other contained 50ml sodium borohydride (100mM). The synthesis reaction was initiated by the addition of sodium borohydride to the copper ions solution, followed by stirring for 40 min. The color changed as reported in the literature (Wu and Chen 2004), and the appearance of wine-red color of the high concentration copper nanoparticles indicated the reduction reaction has completed.

### **2.2.3 Dialysis process**

After formation of Cu-NPs, the suspension was dialyzed in the dialysis tubing (Nominal MWCO of 3,500Da, fisher brand) for 24hr to remove the undesired salts, excess reducing agent and unreacted capping agent. When preparing the dialysis tubing, it was determined that for 100ml solution, 90 cm long dialysis tube was ideal for the desired capacity of 1.15ml/cm. The tubing was first dipped in the DI water for 20min for its expansion. Then the solution was poured into the tube with one end tightened by a blue clip. After loading all the solution, the other end of the dialysis tubing was tightened by a blue clip as well. The whole tubing should be immersed in the DI water under stirring for 24 hr. During the dialysis procedure, the DI in the big container needed to be changed at least four times periodically to ensure the effectiveness of dialysis. The conductivity of the water outside of the tube was also measured to detect the completion of dialysis process. Finally, the

suspension solution was poured into a capped bottle and stored at 4 °C. The Cu-NPs suspension needed to be sonicated before use.

## **2.3 Attachment of the Cu-NPs to the TFC membranes**

### **2.3.1 Electrostatic method**

The attachment of CuNPs onto the TFC membrane via electrostatic method is achieved by immersing the PA functional layer into the Cu-NPs suspensions for 24 h. The electrostatic bonding was achieved during the contact between the positively-charged Cu-NPs suspension (20 ml) and negatively-charged TFC membrane. The Cu-NPs suspension needed to be sonicated (Branson model 2510) for 10 min to get a well-dispersed status. After the contact for 24h, the membrane was rinsed three times with DI water to remove the unbound Cu-NPs. The CuNPs-functionalized membrane with the electrostatic method was labeled as TFC-Cu-NPs, and stored in DI water at 4°C before test.

### **2.3.2 Covalent chemical bonding**

Cysteamine ( $\text{H}_2\text{N}-(\text{CH}_2)_2\text{-SH}$ ,  $\geq 98.0\%$ ) was obtained from Sigma-Aldrich. Ethanol was purchased from Decon Laboratories, Inc. Cysteamine and ethanol solution was used to functionalize the PA active layer first to introduce the thiol groups. After the interfacial polymerization reaction, the membrane was rinsed with pure hexane. Instead of drying the membrane at 80 °C, the membrane was immediately rinsed with ethanol and immersed in a cysteamine-ethanol solution (20 mM, 50 ml) for 24h. The membrane (labeled as TFC-SH) was then rinsed with pure ethanol and DI water, ready for further functionalization with Cu-NPs via covalent bonding.

The Cu-NPs suspension needed to be sonicated (Branson model 2510) for 10 min to get a well-dispersed status. After being functionalized with thiol groups, the membrane surface was immersed with the Cu-NPs suspensions for 24 h. The membrane, labeled as TFC-S-CuNPs, was then rinsed three times with DI water to remove the unbound Cu-NPs, and stored in DI water at 4°C before test.

## **2.4 Characterization of the Cu-NPs**

### **2.4.1 Transmission electron microscopy (TEM)**

TEM (JEOL, 1400, JEOL Ltd., Peabody, MA) was used to observe the morphology and general particle size. TEM samples of Cu-NPs were prepared by putting a droplet of Cu-NPs suspension-ethanol solution onto the carbon coated copper grid and then drying at the room temperature. Ethanol could help accelerate the drying procedure with negligible effect on the sample. To disperse the nanoparticles for better imaging, the Cu-NPs in ethanol at a low concentration was sonicated for 1hr. Image J software was used to analyze the size distribution and mean diameter of the Cu-NPs based on the TEM images.

### **2.4.2 Zeta potential analysis**

The surface charge of the synthesized Cu-NPs was a critical factor in determining the attachment effect via the electrostatic interactions. Moreover, considering the membrane fouling, it was generally considered that the membrane surface with near neutral condition had better anti-fouling properties. Accordingly, it was meaningful to evaluate the zeta potential of the synthesized nanoparticles.

Zeta potential of the Cu-NPs suspension solution was assessed by a zeta potential analyzer (Zetasizer, Malvern) in this study. Samples of the Cu-NPs suspensions were prepared under different pH values from 4 to 11, adjusted by nitric acid and ammonia solution. Every sample was measured for three times to ensure data repeatability and accuracy.

## **2.5 Modified TFC membranes characterization**

### **2.5.1 Water contact angle**

The hydrophilicity of the membrane surface could be determined through the surface contact angle measurement with DI water. If the surface is hydrophilic, the water droplet could easily spread on the dense surface and the angle between the wet surface and the outline of droplet should be low. If the surface is hydrophobic and hard for water to spread, the water droplet stayed like a partial ellipse and the contact angle would be high.

The water contact angle in this study was measured by the sessile drop method on a standard contact angle goniometer. The membrane sample was fixed on a flat glass with tapes to ensure the membrane was horizontal.

### **2.5.2 Scanning electron microscopy (SEM)**

SEM (FEI Quanta 600 FEG) with Energy-dispersive X-ray spectroscopy (EDS) analysis was conducted to observe the surface morphology and the elements existed on the TFC membrane. A small piece of the dry membrane sample was placed onto the holder and

sputter-coated with Platinum (20mA, 30s). The images were taken at various magnifications at 25kv under the pressure of  $4 \times 10^{-4}$ psi.

### 2.5.3 Attenuated total reflectance Fourier transform infrared spectroscopy (ATR-FTIR)

ATR-FTIR (Nicolet 4700 FTIR, Thermo Electron Corp., Waltham, WA) was used to evaluate the functional groups on membrane surface. All spectra images contained the wave numbers from  $500\text{-}4000\text{ cm}^{-1}$  with 128 scans at a resolution of  $1.0\text{ cm}^{-1}$ . The ATR accessory was fixed at the angle of  $45^\circ$ .

### 2.5.4 Reverse osmosis process

The reverse osmosis testing apparatus was set up according to the schematic diagram below (Fig 2.1). Details of this high pressure cross-flow filtration system was described in Yin's previous work (Yin, Kim et al. 2012).

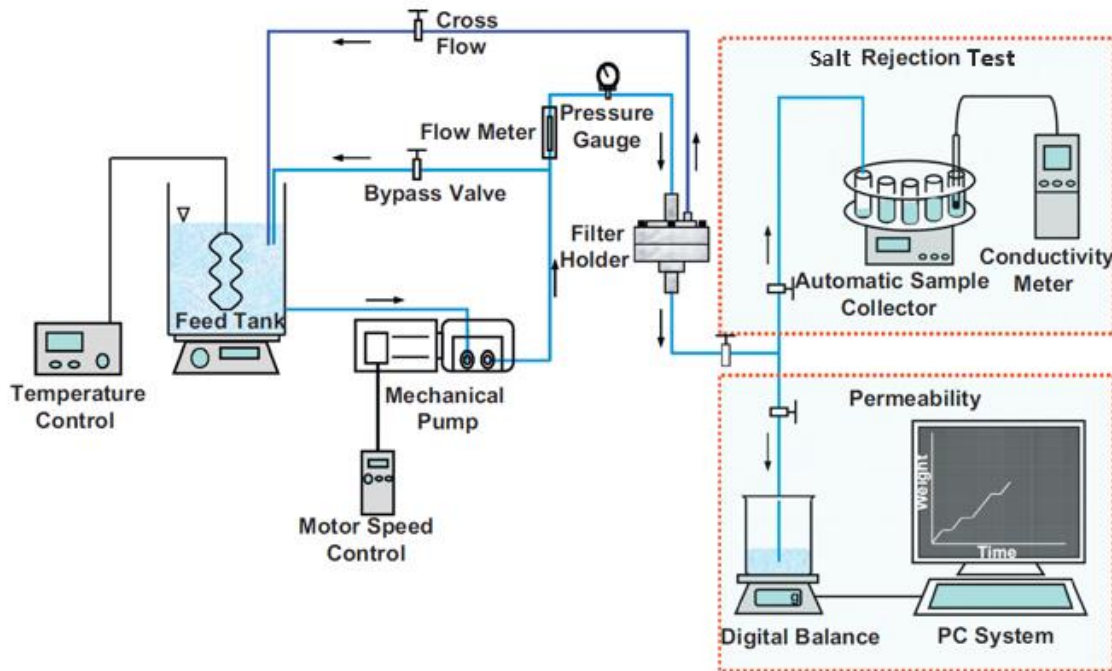


Fig 2.1 The schematic diagram of reverse osmosis filtration system

The prepared flat sheet TFC membrane was tailored to 9.6 cm<sup>2</sup> as the effective area to fit the filter holder. After installing the membrane unit, the reverse osmosis filtration began under the control of a motor. The pressure gauge could be adjusted to the desired value by adjusting the bypass valve and cross flow valve. The feed tank temperature was controlled at 25 ±1 °C by a circulation system. The permeate solution was collected, weighed and recorded by the Lab View automated data recording system.

The water flux under the certain pressure was calculated by the equation 2.1 below. After testing the flux, the conductivity of the feed and permeate was measured by a conductivity/TDS meter (HACH Company, Loveland, CO) respectively. The rejection rate could be calculated based on these data, as described by equation 2.2.

$$J = \frac{V_p}{A * t} \quad (2.1)$$

$$R = \left(1 - \frac{C_p}{C_f}\right) * 100\% \quad (2.2)$$

Where,

J --- Water flux (L/m<sup>2</sup>h)

V<sub>p</sub>--- Volume of the permeate water (L), 0.001×weight of permeate (g), ρ is 1g/1mL.

A--- Effective area (m<sup>2</sup>)

t--- Filtration time (h)

R--- Salt rejection

$C_p$ --- Salt concentration of permeate solution, proportional to the conductivity of the permeate

$C_f$ --- Salt concentration of feed solution, proportional to the conductivity of the feed solution

For pure water flux test, the feed container was filled with DI water. The membrane was compressed at 300 psi for 3 h to reach a steady state. This test is basically to observe the water flux performances with pressure as the only variable (100, 200, 300, 400, 500 psi). For the desalination test, 4g sodium chloride (Sigma-Aldrich) was dissolved in 2L DI water. The concentration of the feed solution was 2000mg/L. The desalination process was also carried out under the pressure of 300psi.

### **2.5.5 Anti-bacterial assessment**

The anti-bacterial tests conducted with the bacteria *P. aeruginosa*. *P. aeruginosa* PAO-PR1 (ATCC<sup>®</sup> 39018<sup>™</sup>), which is an opportunistic pathogen and a model microorganism for proteobacterial biofilm study (Klausen, Heydorn et al. 2003, Irie, Borlee et al. 2012), was purchased from American Type Culture Collection (ATCC) and stored at -80 °C in 10vol.% glycerol solution (Fisher Scientific) (Tipton, Coleman et al. 2013). Before each experiment, it was freshly plated from the frozen stock on Luria Bertani (LB) agar plates (Fisher Scientific) (10 g/L of casein peptone, 5 g/L of yeast extract, 5 g/L of sodium chloride, and 15 g/L of agar as final concentrations) and incubated at 34 °C for overnight. Subsequently, one single colony was transferred into LB Broth (Fisher Scientific) (10 g/L of casein peptone, 5 g/L of yeast extract, and 5 g/L of sodium chloride as final

concentrations) (Ellis, Leiman et al. 2010, Zhang and Hu 2013) and incubated at 34 °C with shaking at 160 rpm.

To measure the antimicrobial activities of the as-prepared membranes, disk experiments were conducted to directly compare and observe the growth of the bacteria. Cell culture of *P. aeruginosa* was diluted serially (by 10 times) using 1×Phosphate-Buffered Saline (1×PBS) (8.00 g/L of sodium chloride, 0.20 g/L of potassium chloride, 1.44 g/L of disodium hydrogen phosphate, and 0.24 g/L of monopotassium phosphate as final concentrations) (Camassola, de Macedo Braga et al. 2012) and aliquots (100 µL) of the diluted cell culture were spread on LB agar plates. Then, membranes were carefully placed on the surface of the LB agar plate (upside-down), letting the surface of functional layer in contact with the bacteria-agar surface. The plates were incubated for overnight (34 °C) before checking the growth of cells. After incubation, the membrane was carefully peeled off and both the membrane surface and the colony area were examined to see the growth of *P. aeruginosa*.

Also, samples for SEM investigation were prepared to observe the activity and aliveness of *P. aeruginosa*. The cell culture of *P. aeruginosa* was diluted using 1×PBS to a final cell density of ~10<sup>6</sup> cells/mL in a 50-mL plastic tube. A piece of membrane (1 cm<sup>2</sup>) was soaked in the cell culture with shaking at 100rpm for 6 hr at room temperature. Then the membrane sample with cell incubated was immersed in 3 vol. % glutaraldehyde (GA)-PBS solution for 5h at 4°C. After the bacteria were fixed onto the membrane surface, the membrane sample was rinsed with PBS solution three times to remove the remaining GA solution. Finally, a series of ethanol solution were used to dehydrate the membrane

gradually from 25% to 100%. The dry membrane samples were examined by SEM following the method described in chapter 2.5.2.

## CHAPTER THREE

### RESULTS AND DISCUSSION

#### 3.1 Cu-NPs synthesis and characteristics

##### 3.1.1 Synthesis of Cu-NPs

Cu-NPs synthesized to functionalize the thin film composite membranes need very specific characteristics to successfully introduce the antibacterial properties for RO desalination systems. The nanoparticles must be inexpensive, easily synthesized, simple to be affiliated with the membrane surface, and meanwhile able to maintain or even improve the membrane performance. All these constraints of Cu-NPs were considered in this study.

For the synthesis of Cu-NPs through cupric ion reduction by sodium borohydride, appearances of various solutions and reaction products are shown in Figure 3.1. NaBH<sub>4</sub>-CTAB solution was light gray (Fig 3.1A) and CuCl<sub>2</sub>-CTAB solution was light blue (Fig 3.1B). The addition of NaBH<sub>4</sub> to copper ions solution caused an immediate change of color to yellowish brown indicating the formation of metallic Cu-NPs wrapped by the CTAB layers (Fig 3.1C). After cleaning by dialysis for the removal of unreacted species, especially the NaBH<sub>4</sub> and CTAB, the color became comparatively pure reddish brown (Fig 3.1D).

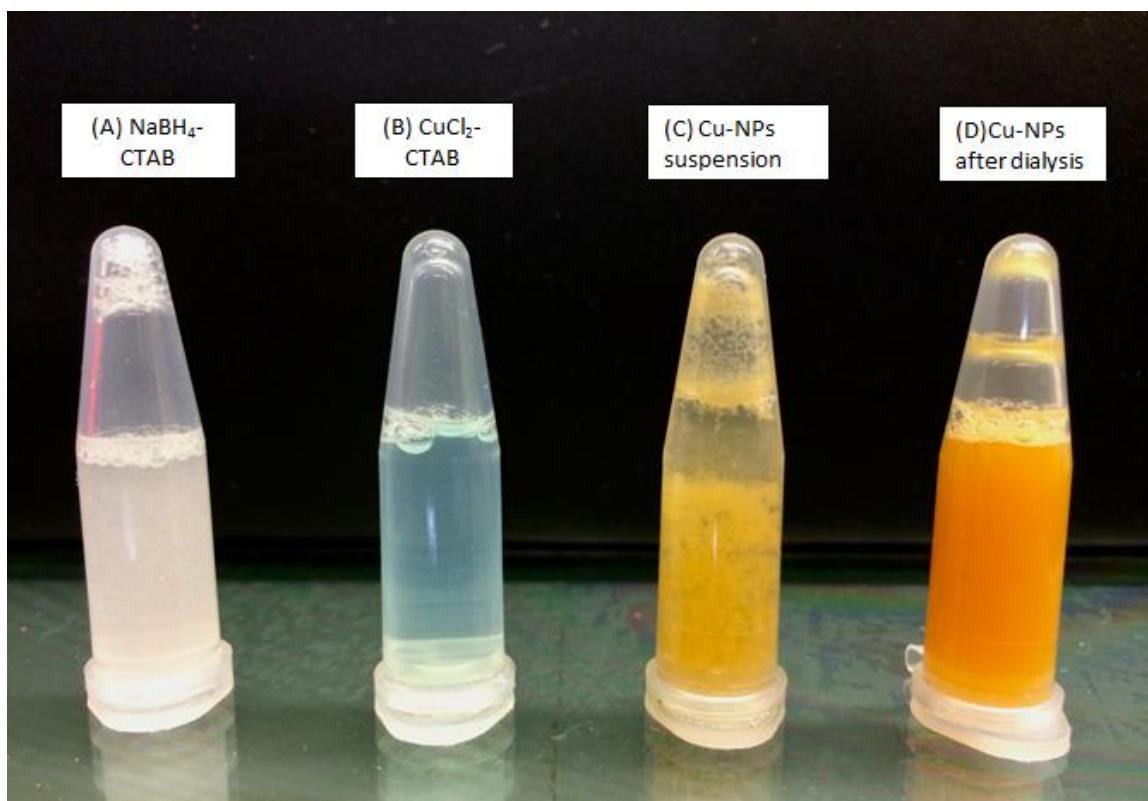


**Fig 3.1 Cu-NPs preparation procedure with color changes**

It was notable that in Fig 3.1 (c), some aggregates of Cu-NPs were observed. It is likely that with a high concentration of salt, the positively-charged electrical double layer was compressed causing the particles to aggregate. After the dialysis that removed unreacted CTAB and salts, the electrical double layer extends a longer distance so the particles are better dispersed (Fig 3.1 (d)).

The Cu-NPs suspension was stored in a capped bottle at 4 °C. No oxidation was found for at least a month, only some particle precipitation. Ultrasonic treatment was conducted every time before the use of the Cu-NPs to membrane modifications.

The Cu-NPs were synthesized with cetyl trimethylammonium bromide ((C<sub>16</sub>H<sub>33</sub>)N(CH<sub>3</sub>)<sub>3</sub>Br, CTAB) as a capping agent in this study. The capping agent plays a

critical role, which can not only prevent particle agglomeration but also bring the positive charge to the surface of the nanoparticles so the CuNPs could be attached to the negatively charged polyamide thin layer through electrostatic attractions.

### 3.1.2 Mean diameters of the Cu-NPs

To determine the mean diameter and morphology of the Cu-NPs, transmission electron microscopy (TEM) was used to acquire the images of the dispersed Cu-NPs (Figure 3.2). The distribution of the nanoparticles was then analyzed via Image J program (Figure 3.3).

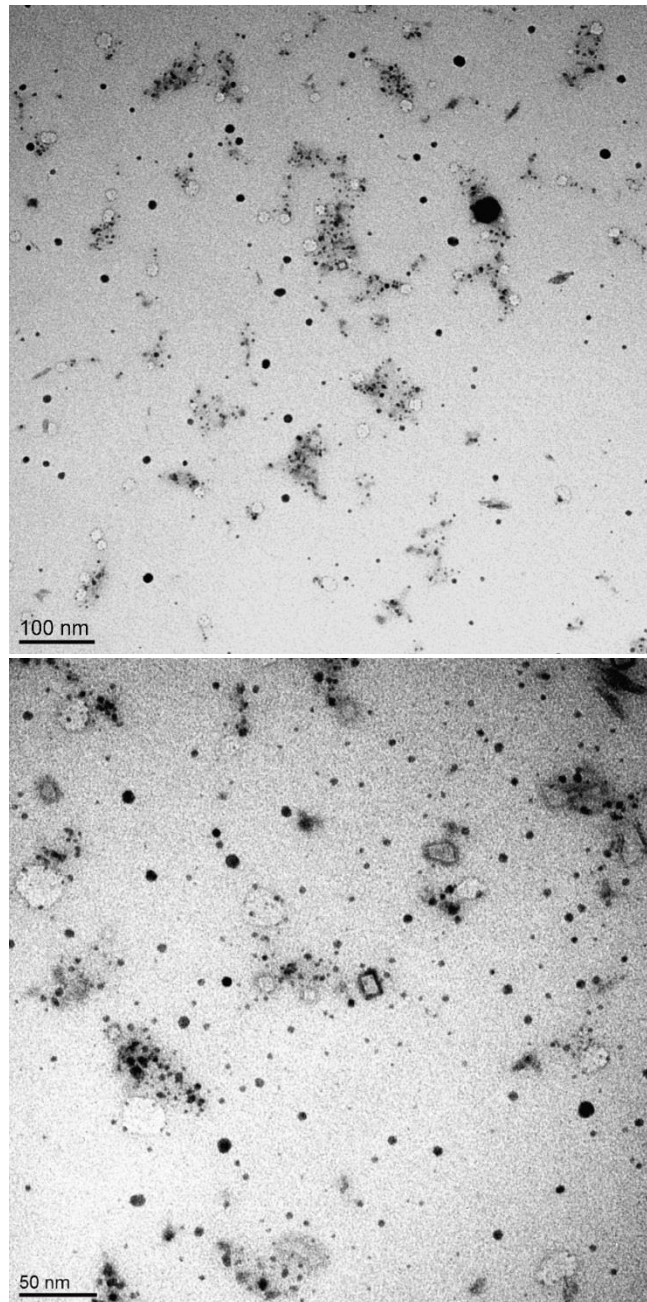
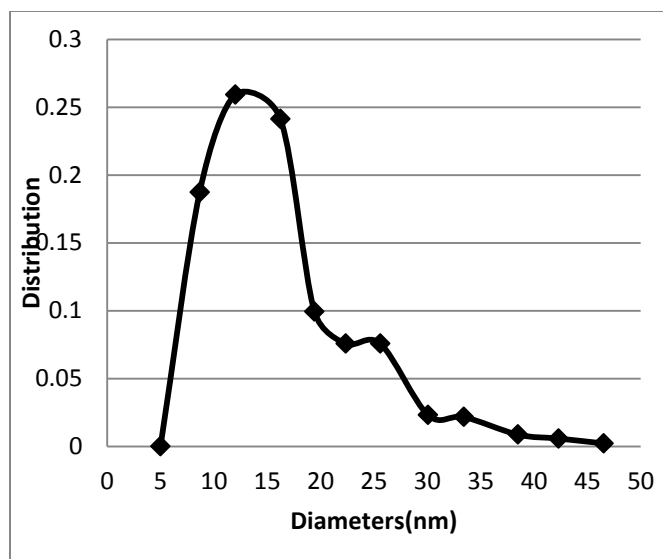


Fig 3.2 TEM image of Cu-NPs suspension solution with the scale of 100nm and 50nm



**Fig 3.3 Distribution of Cu-NPs of different diameters (nm)**

Among the 1388 points collected from three different TEM images, 26% of the nanoparticles were of 12nm; 24% were of 16.2nm; 18.7% were of 8.7nm. The analysis results confirmed that the diameters of most Cu-NPs were in the range of 9-20 nm, with the mean diameter of 15.31nm.

### 3.1.3 Zeta potential of Cu-NPs

It is known that the polyamide surface was slightly negative charged due to the functional group of carboxylic acid. When preparing the copper nanoparticles, CTAB was used as a cationic surfactant that brings positive charges to the metallic copper nanoparticles. The charge on the Cu-NPs decreases with increasing solution pH, as indicated by the zeta potential measured in the pH range from 5.0 to 11.2 (Fig 3.4). In the whole pH range tested, however, the charge is always positive.

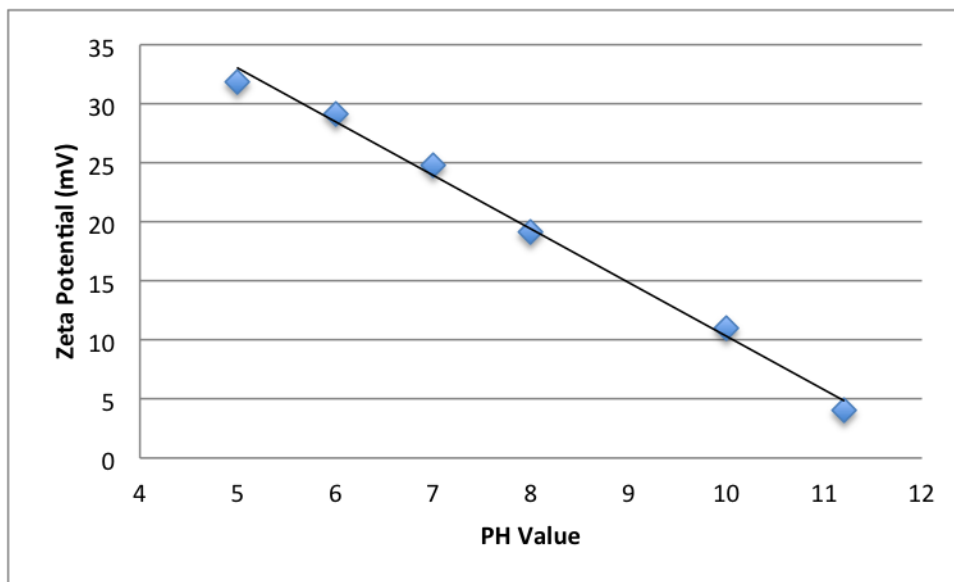


Fig 3.4 Zeta potential of Cu-NPs at different PH values (5.0-11.2)

## 3.2 Membrane properties

### 3.2.1 Contact angles

The hydrophilicity of the membrane surface could be investigated by measuring the water contact angle. In this research, the contact angles of various membranes were tested with DI water (Figure 3.5). The membranes from left to right is the pristine TFC membrane, the membrane with S-H functional group (TFC-SH), the membrane with Cu-NPs attached via electrostatic interactions (TFC-CuNPs), the membrane with the covalent bound CuNPs (TFC-S-CuNPs), and the membranes after being applied for desalination test (TFC-CuNPs (after) and TFC-S-CuNPs (after)).

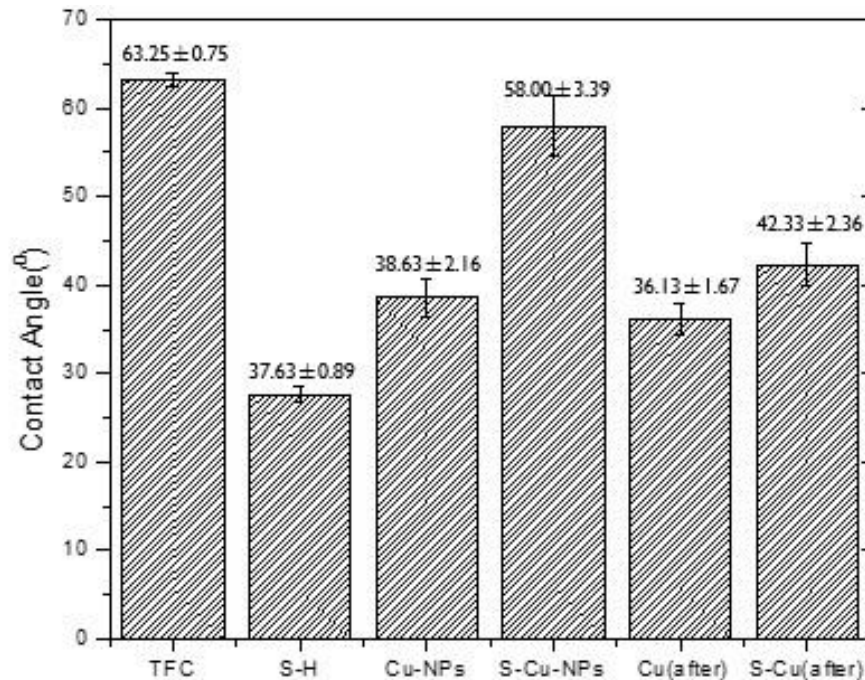


Fig 3.5 Water contact angle of different membrane surfaces

The contact angle measurement results indicated that in comparison with the pristine TFC membranes, the contact angles for all other membrane surfaces were smaller, indicating that the modified membranes were more hydrophilic. The water contact angle is

63.25±0.75° for TFC membrane, 37.63±0.89° for THC-SH, 38.63±2.16° for TFC-CuNPs, 58.00±3.39° for TFC-S-CuNPs, 36.13±1.67° for TFC-CuNPs after desalination test and 42.33±2.36° for TFC-S-CuNPs after the desalination test.

The TFC-SH with a low water contact angle could be explained by the introduction of hydrophilic thiol (-SH) functional group. The membrane was immersed in ethanol solution for hours and washed by the pure ethanol afterwards during the functionalization process, which enabled the membrane swelling to some extent and may have also contributed to the enhanced hydrophilicity. In the TFC-S-Cu membrane where the thiol group was neutralized by forming the thiol-metal coordination, the contact angle became higher but still lower than the pristine TFC membrane. With the incorporated Cu-NPs by electrostatic interactions, the TFC membrane surfaces became rougher and allowed better spreading of water so the contact angle was significantly lower than the pristine membrane. The results were consistent with other researches that immobilized nanoparticles (Zodrow, Brunet et al. 2009, Prabhawathi, Sivakumar et al. 2012, Yin, Yang et al. 2013). After the membranes were applied for desalination tests, the contact angles remained lower than the pristine membranes.

### 3.2.2 SEM images of membranes loaded with Cu-NPs

Fig 3.6 showed the membrane surface under the SEM was immersed in cysteamine/ethanol solution for 24hr, followed by washing by pure ethanol, which may have caused the swelling structure observed on the surface.

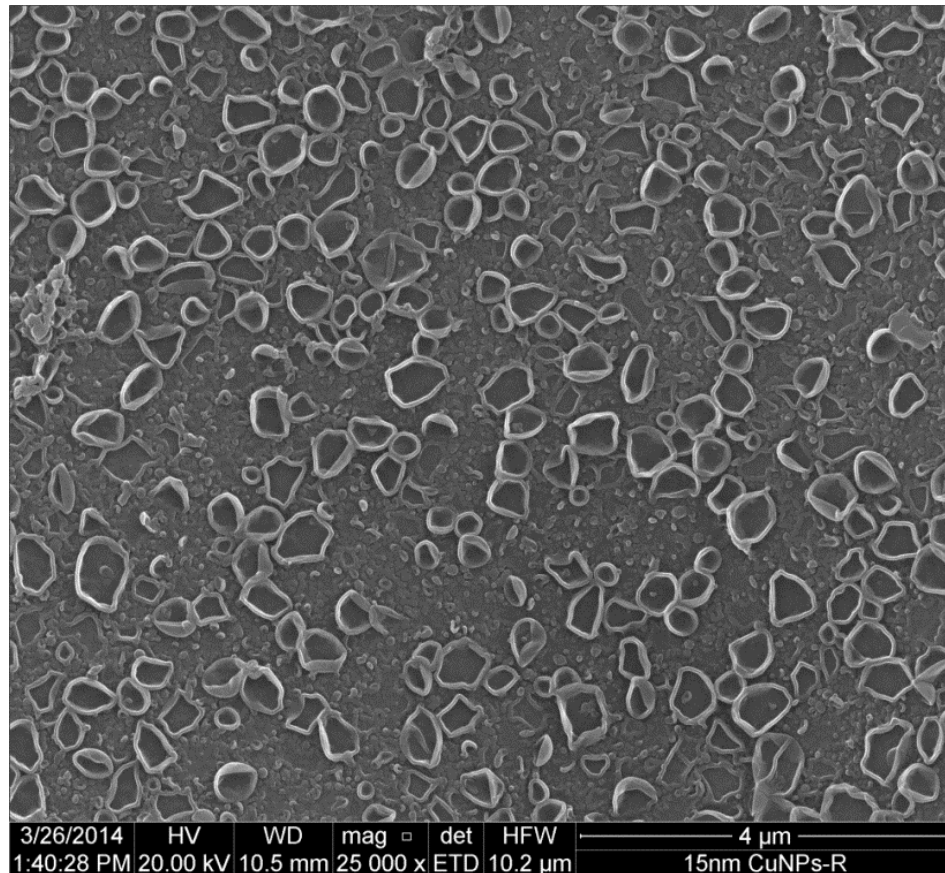
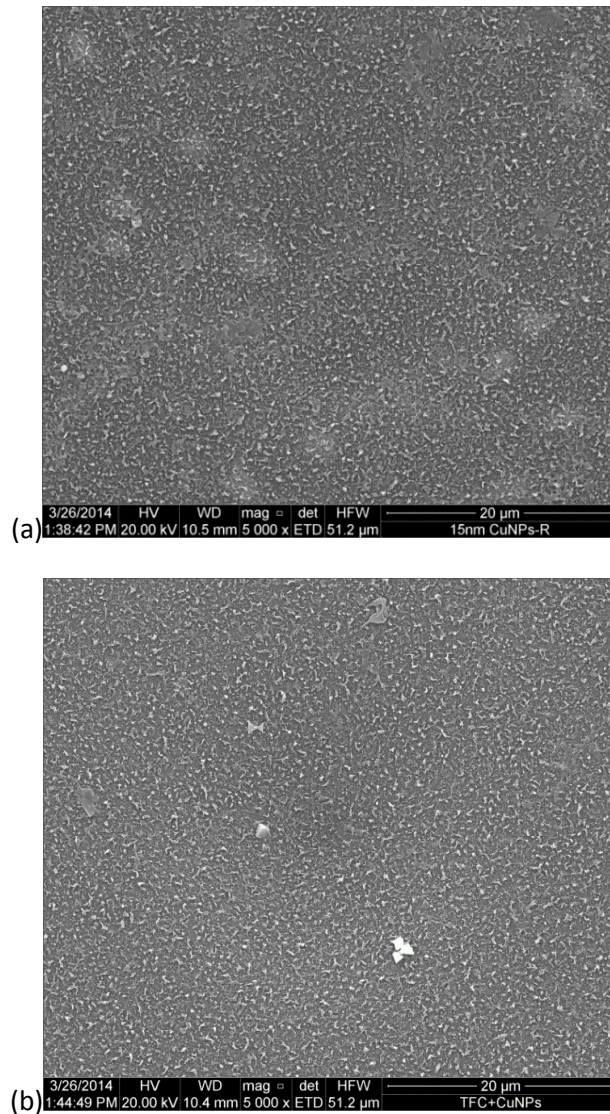


Fig 3.6 SEM image of the membrane after immersing in the cysteamine/ethanol solution for 24hrs

Fig 3.7- Fig 3.10 illustrated the morphology of the TFC membranes via electrostatic and covalent bonding. Under a relatively low resolution ( $\times 5,000$ ), the surface of the modified membranes was similar to the pristine TFC membrane surfaces. The Cu-NPs with an approximately 15nm could not be observed at this resolution. At a higher resolution ( $\times 50,000$ , Fig 3.8), a large number of Cu-NPs could be observed on the membrane surfaces.



**Fig 3.7 SEM surface morphology of Cu-NPs incorporated TFC membrane. (a) is fabricated via electrostatic method TFC-CuNPs; (b) is made via covalent bonding TFC-S-CuNPs.**

Fig 3.8(a)TFC

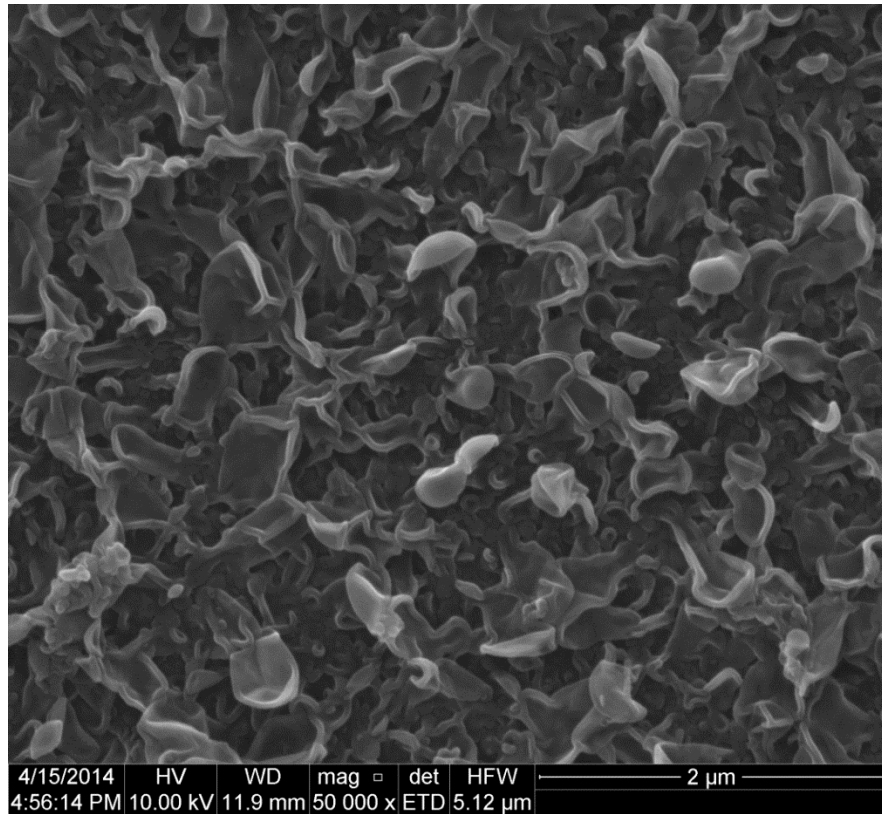


Fig 3.8(b) TFC-CuNPs

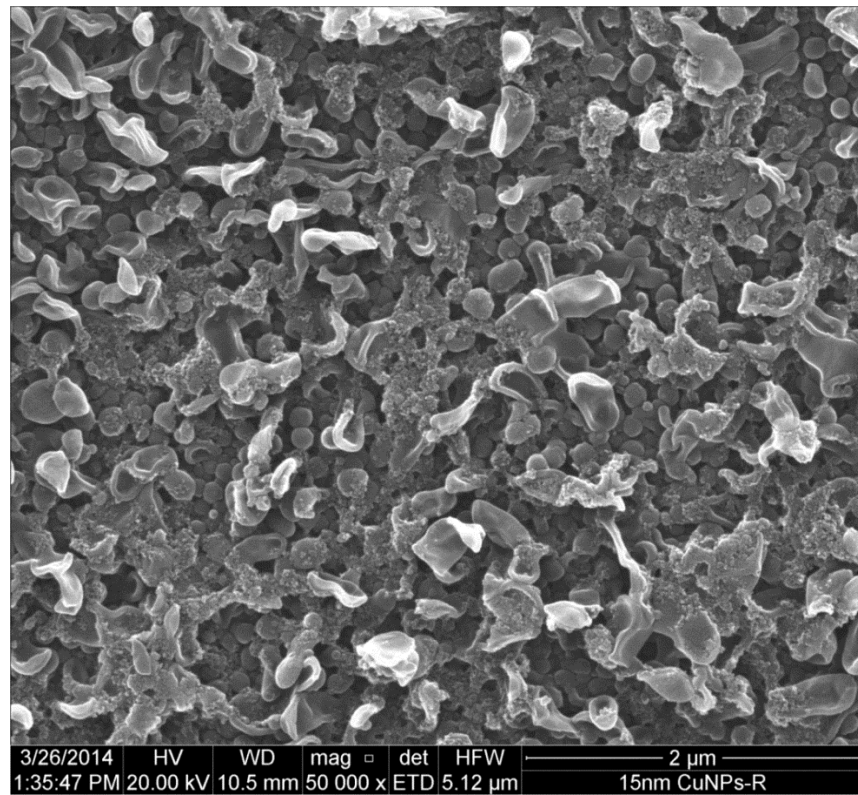


Fig 3.8 (c) TFC-S-CuNPs

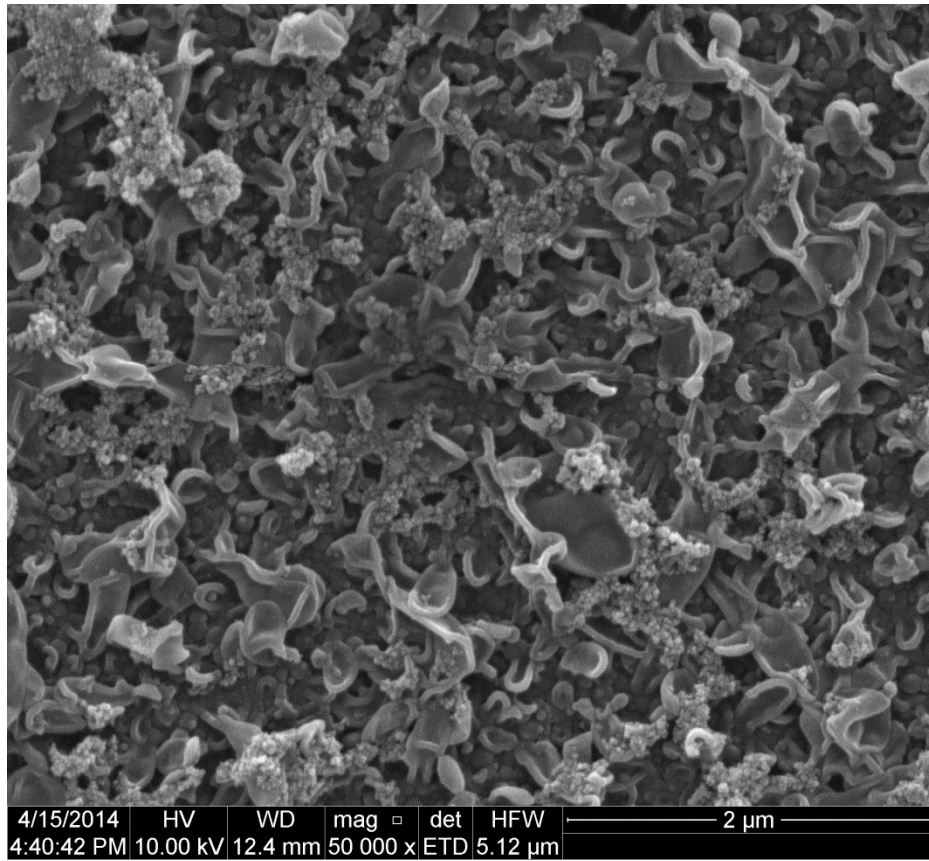
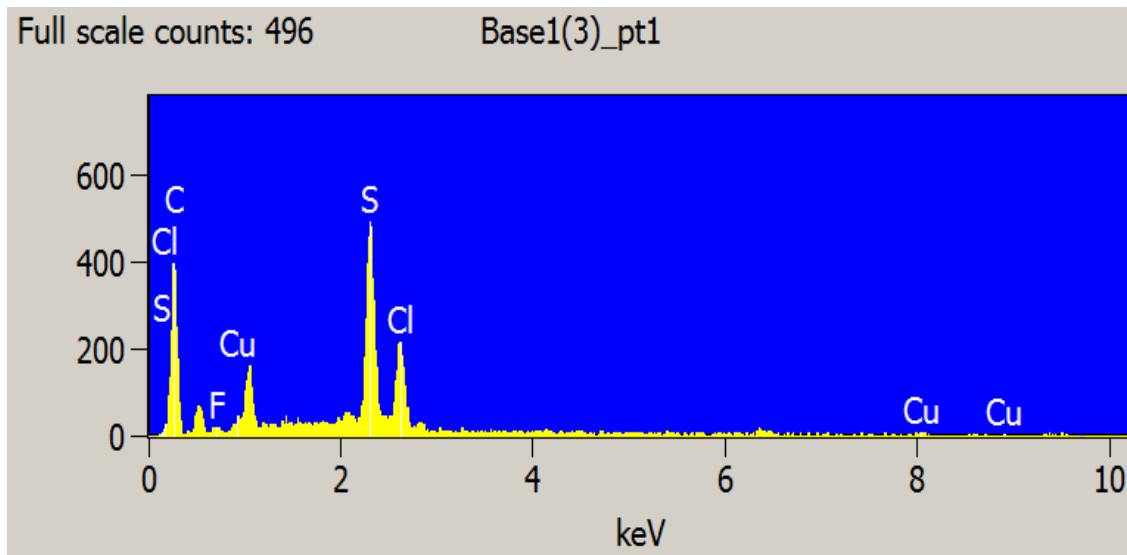
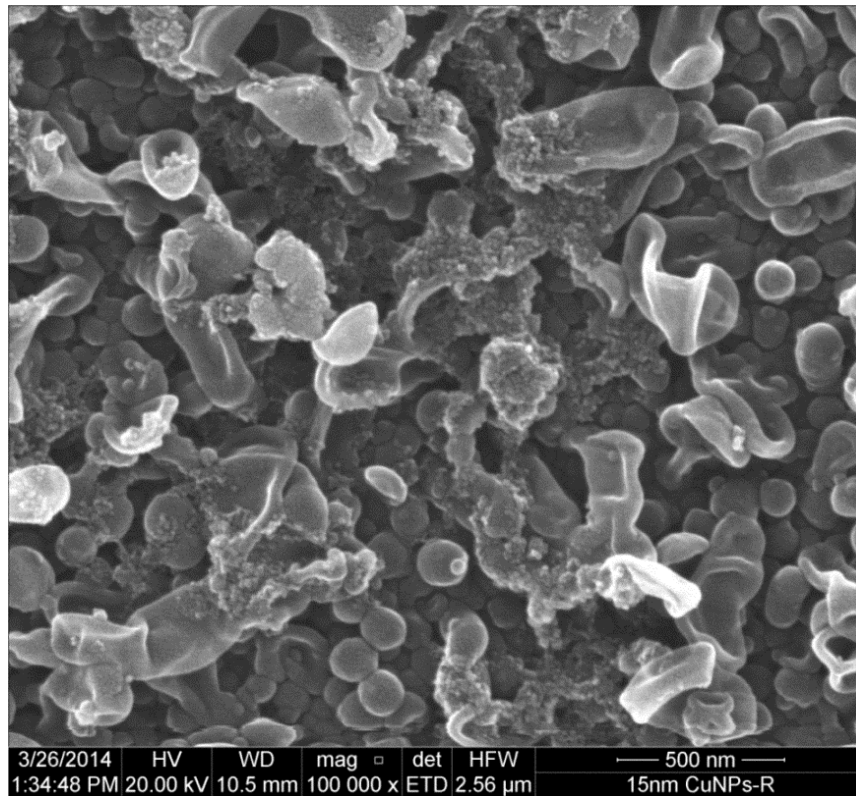


Fig 3.8 Bigger magnifications with detailed the structure of the membrane surface: (a) TFC  
(b) TFC-CuNPs (c) TFC-S-CuNPs

To confirm that the existence of copper in the structure, EDS analysis (Fig 3.9) was conducted showing copper is one of the major elements on the membrane surfaces.



**Fig 3.9 EDS test to analysis the elements existed on the surface of the Cu-NPs incorporated membranes**

The SEM images (Fig 3.10) also showed that CuNPs were still on the surfaces after the membrane was applied for the desalination tests.

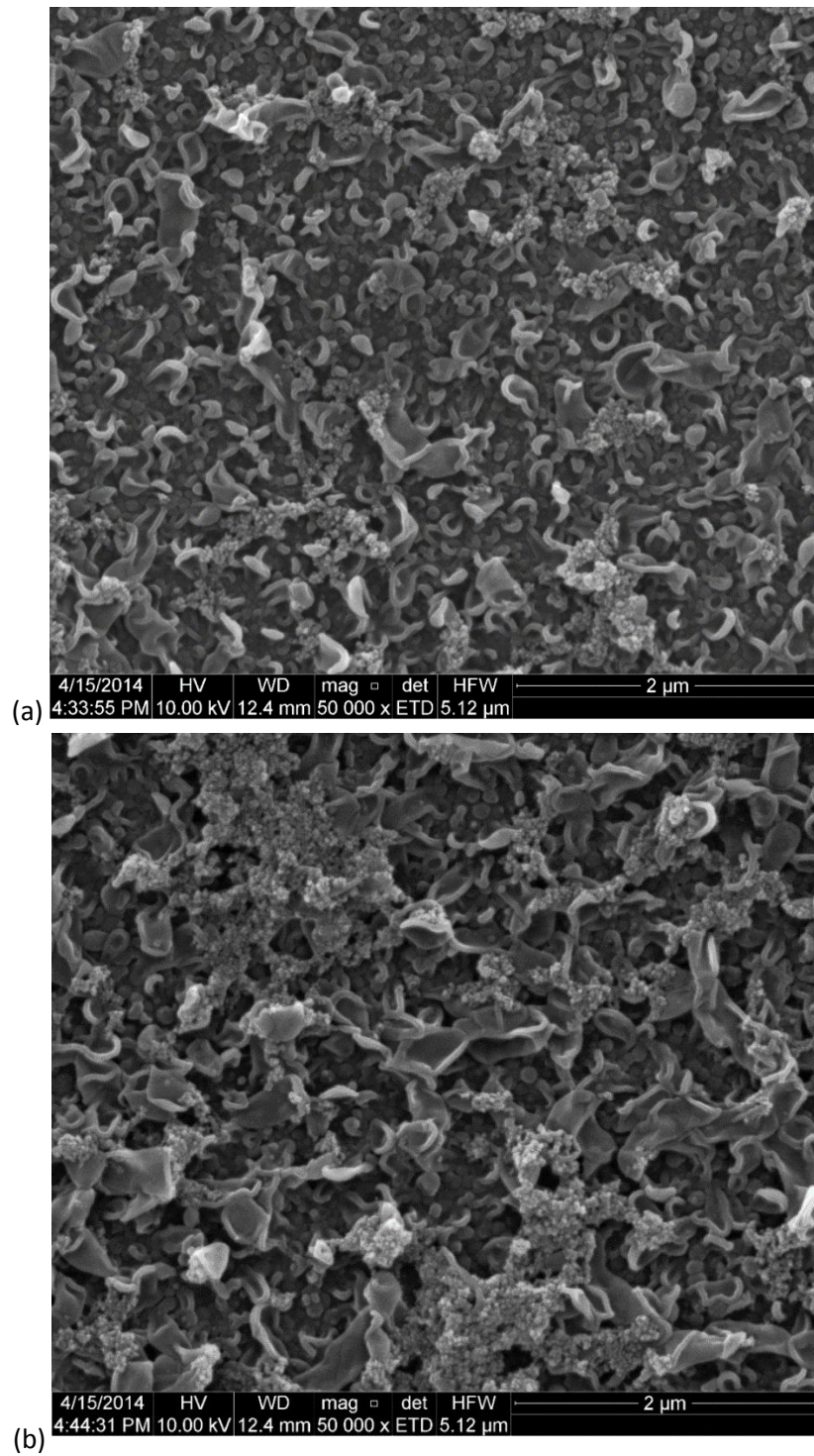


**Fig 3.10 SEM images of the (a) TFC-CuNPs (b) TFC-S-CuNPs membranes after the desalination test**

### 3.2.3 ATR-FTIR spectra analysis

The ATR-FTIR spectra of TFC, TFC-CuNPs, TFC-SH and TFC-S-CuNPs were presented in Figure 3.11. The unchanged peaks after membrane modifications were 1660  $\text{cm}^{-1}$  (amide I, C=O stretching vibrations of amide), 1610  $\text{cm}^{-1}$  (N-H stretching of amide), 1547  $\text{cm}^{-1}$  (amide II, in-plane N-H bending and C-N stretching vibrations), and 1450  $\text{cm}^{-1}$  (C=O stretching and O-H bending of carboxylic acid) (Lee, Im et al. 2008, Tarboush, Rana et al. 2008, Yin, Yang et al. 2013). The peak at 768  $\text{cm}^{-1}$  (C-Cl stretching) slightly decreased after functionalizing with cysteamine (Parada, de Almeida et al. 2007). However, the peak at 2540-2560  $\text{cm}^{-1}$  (S-H stretching) did not show up (Wharton 1986). This also happened to Yin et al. when they examined the membranes with silver nanoparticles. The main reason could be that: (1) with high polarizability of sulfur, the thiol groups were not sensitive enough to be detected; and (2) small amount of thiol group were attached to the membrane surface (Yin, Yang et al. 2013).

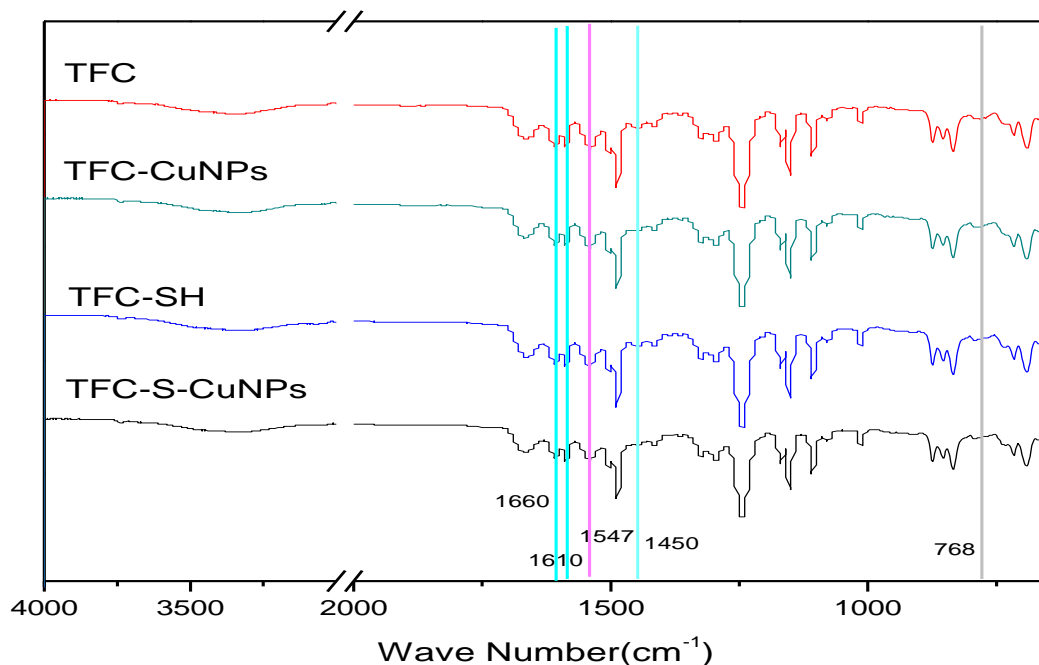


Fig 3.11 ATR-FTIR spectra analysis of the membrane surface

### 3.3 Membrane Performance for Desalination

#### 3.3.1 Pure water test

The relationship between the pure water flux and the operating pressure was described in Fig 3.12. The water flux decreased in order of TFC-SH > TFC-S-CuNPs > TFC-CuNPs > TFC. This order in decreasing water flux is identical to the order of increasing membrane hydrophilicity, as gauged by contact angles, suggesting the importance of membrane hydrophilicity for the water transport through the membrane. Another factor could be membrane swelling. As suggested by Kulkarni et al. (Kulkarni, Mukherjee et al. 1996, Committee 2005), the solution like ethanol could cause the swelling of membrane and removal of some small molecular fragments. With a comparatively loose structure, the water flux could be enhanced.

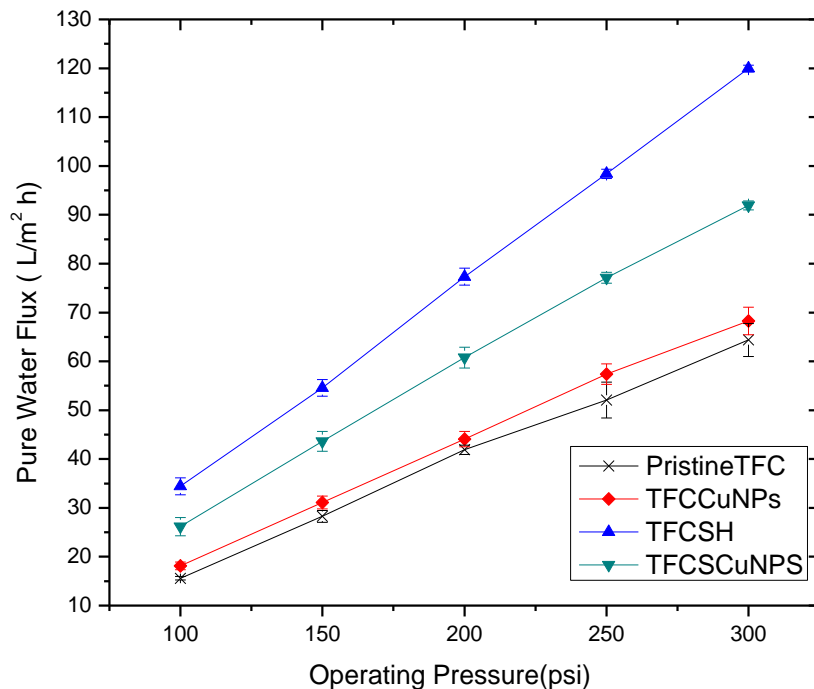


Fig 3.12 Pure water flux of membrane samples

### 3.3.2 Desalination process

The reverse osmosis desalination process was operated under the pressure of 300psi with the feed sodium chloride solution of 2000mg/L. The flux of the membrane decreased at the same order of pure water flux. The water flux was increased from 47.07 L/m<sup>2</sup>h (TFC) to 49.4 L/m<sup>2</sup>h (TFC-CuNPs) and 69.12 L/m<sup>2</sup>h (TFC-S-CuNPs) and the salt rejection was slightly decreased from 94.37% (TFC) to 92.42% (TFC-CuNPs) and 92.26% (TFC-S-CuNPs), respectively.

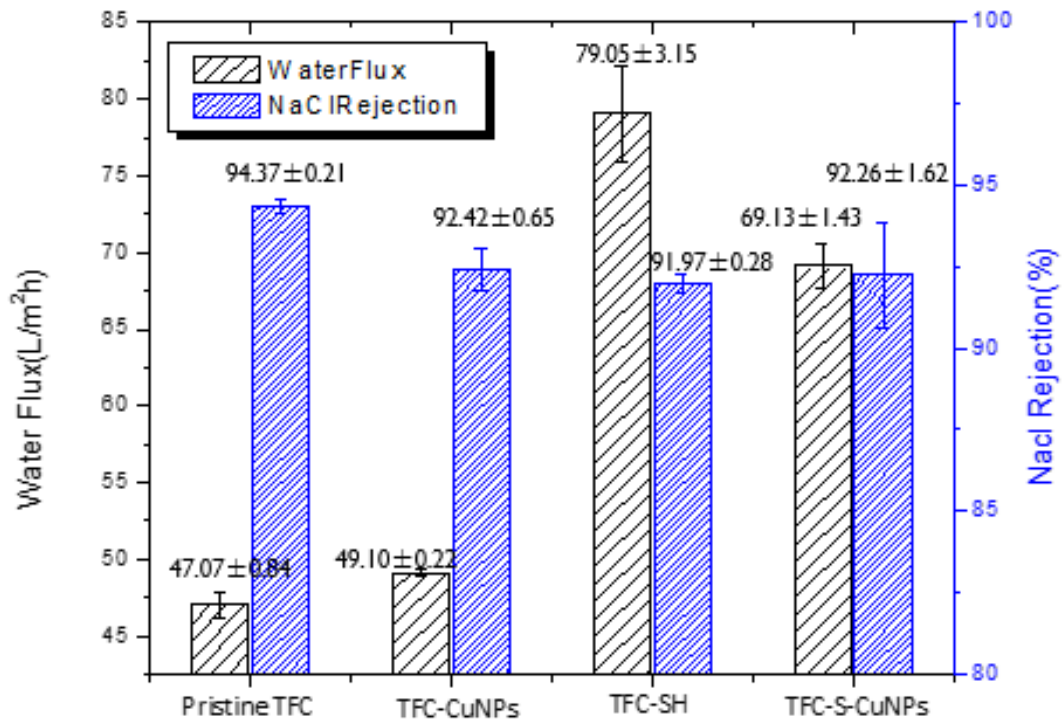
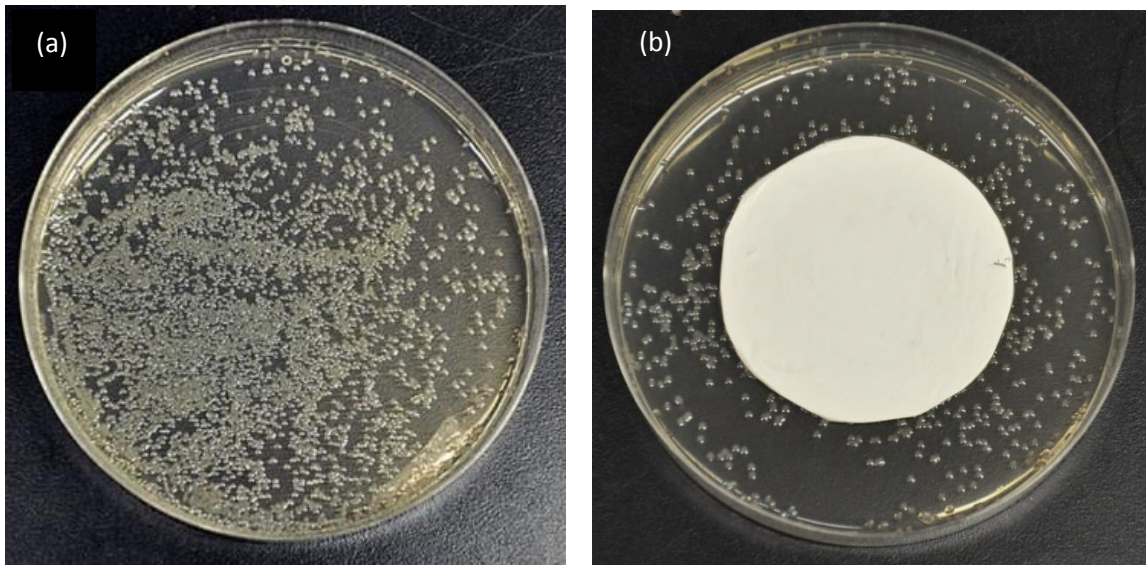


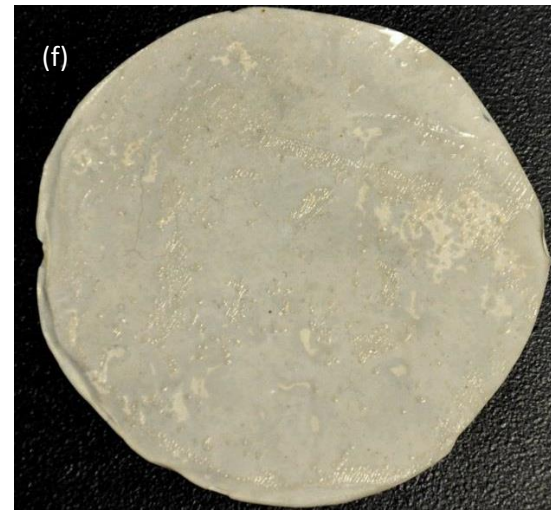
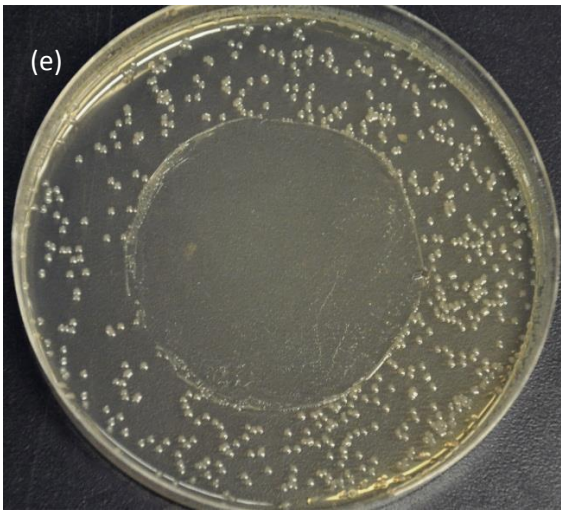
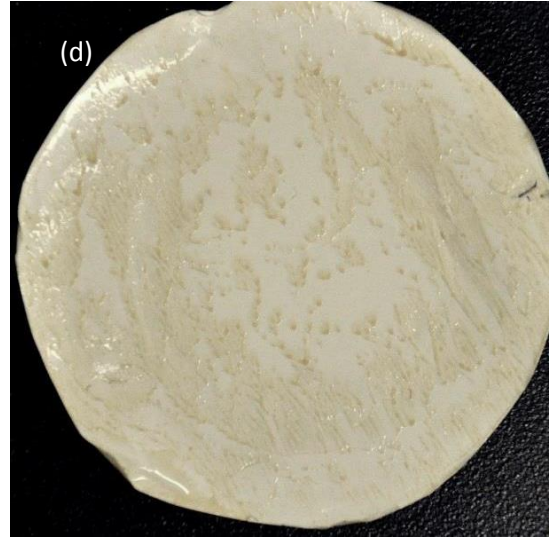
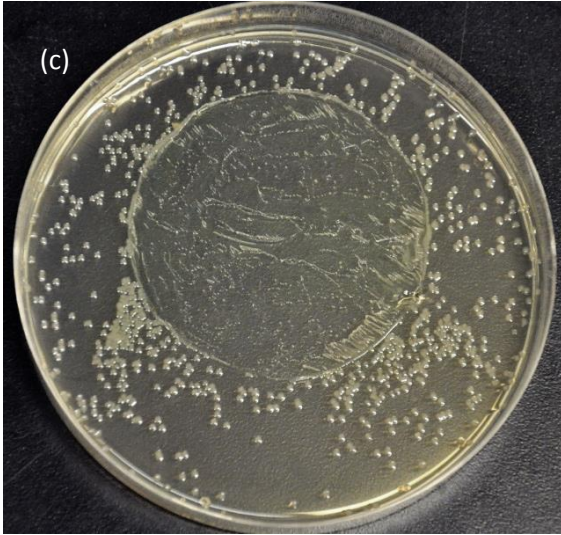
Fig 3.13 Salt rejection and water flux of membrane samples

## 3.4 Antibacterial properties of the membrane surface

### 3.4.1 Disk Tests

*P. aeruginosa* was incubated to investigate the antibacterial properties of membranes. Fig 3.14 (a) showed the normal growth of cell culture on the LB disk; (b) gave an idea of the disk covered with membrane; (C)and (d) revealed that the pristine TFC membrane had no significant anti-bacterial properties. There was *P. aeruginosa* growth not only on the disk but also the surface of the membrane. (e) and (f) showed that TFC-CuNPs could effectively prevent the bacteria growth in the area that covered with the membrane and the membrane surface is comparatively clean. (g) and (h) exhibited the good biocide effect of TFC-S-CuNPs, since the bacteria near the membrane were also affected without growing. A ring-shape colonies of bacteria can be observed on the disk (e) but not on disk (g). Moreover, the membrane surface of the (h) was clean.





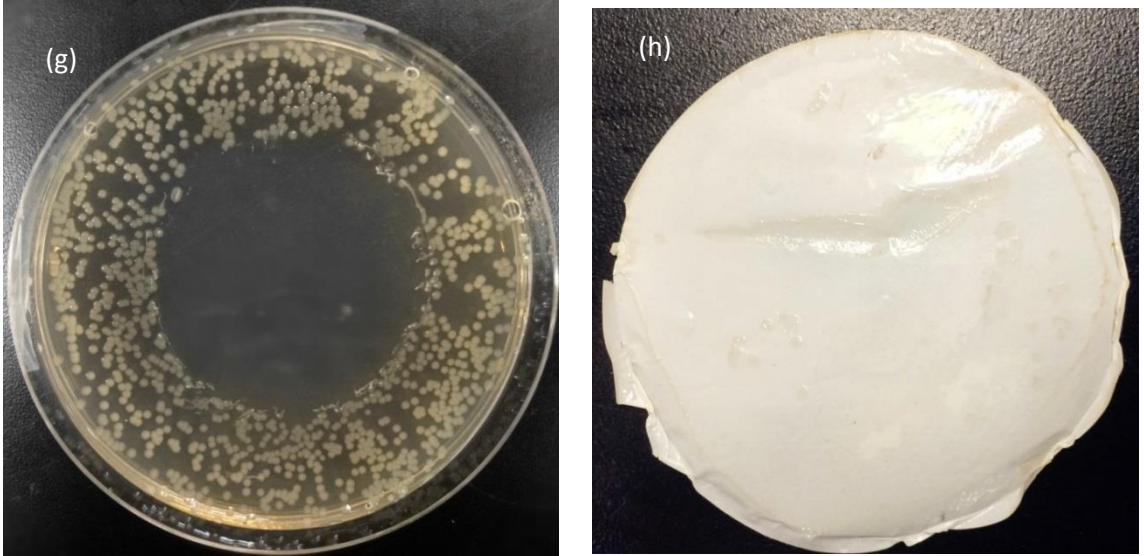


**Fig 3.14 Disk test with *P. aeruginosa* incubation (a) Plain LB disk; (b) TFC surface in contact with the bacteria cell culture before peeling off; (c) colony contacted with TFC; (d) TFC surface; (e) colony contacted with TFC-CuNPs; (f)TFC-CuNPs surface; (g) colony contacted with TFC-S-CuNPs; (h) TFC-S-CuNPs surface**

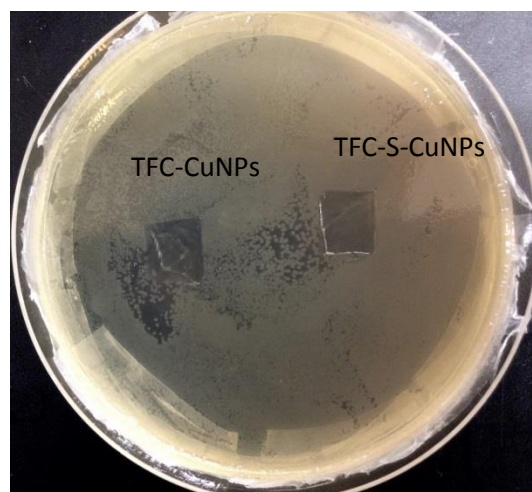


**Fig 3.15 Disk test of *P. aeruginosa* incubation with the left side covered with TFC-CuNPs, the right side covered with TFC-S-CuNPs; The Cu-NPs on both membranes had been released for 7 days**

In order to test and compare the stability of the modified membrane surfaces, the Cu-NPs on both membranes has been released for a week. The 1 cm<sup>2</sup> samples used in Fig 3.15 disk test have been shaken at 100rpm for 7 days in 25ml DI water, with the DI water changed every day. The membranes still showed significant inhibition towards *P. aeruginosa*. The area with the TFC-CuNPs testing coupon had some growth underneath and not with TFC-S-CuNPs, indicating that during the release test, TFC-CuNPs might release copper much more quickly than the TFC-S-CuNPs membranes, so its long term effectiveness is lower.

The Cu-NPs-containing membranes were further treated with nitric acid (HN<sub>3</sub>) to dissolve any remaining copper nanoparticles. The samples of 7 days dissolution were prepared to future copper release evaluations.

### 3.4.2 SEM investigation

Fig 3.16 were SEM images illustrating the bacteria aliveness after shaking with the membranes for 5h. TFC (a) had living *P. aeruginosa* attached to the surface, which was observed as light color and saturated shape. The cells on the membranes containing Cu-NPs were in darker color and flatter in shape. This change was due to the main mechanism of anti-bacterial properties of copper. Generally, the released copper ions caused destroy of cell integrity and leak of cell solute. This experiment also confirmed the anti-bacterial properties of the copper incorporated membrane.

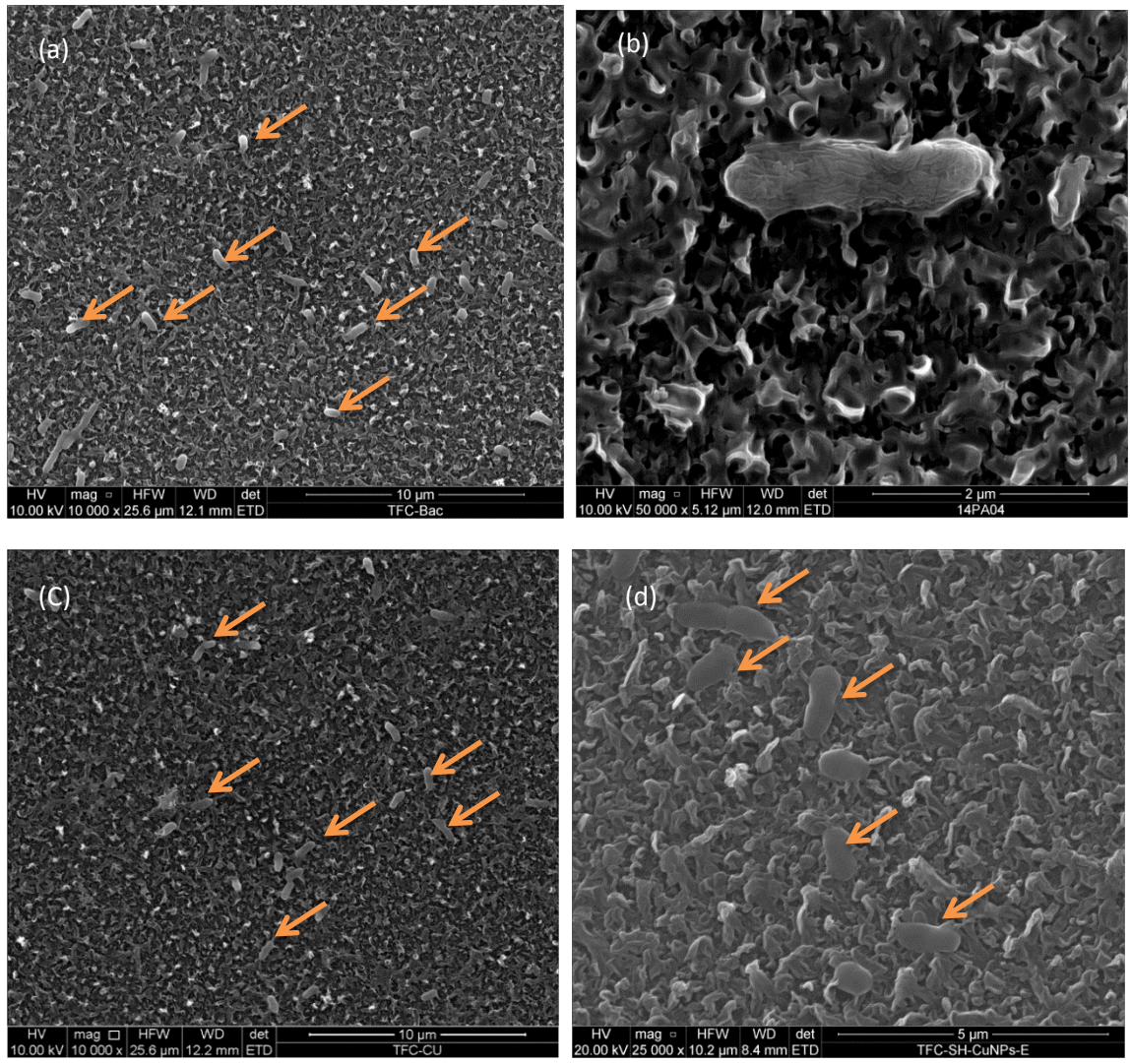


**Fig 3.16 SEM images of membrane surfaces shacked with *P. aeruginosa*-PBS suspension solution for 6h and fixed by GA solution for 5h. (a) TFC (b) alive *P. aeruginosa* (c) TFC-Cu (d) TFC-SH-CuNPs**

## CHAPTER FOUR

### CONCLUSIONS AND FUTURE STUDIES

#### 4.1 Conclusions

The Cu-NPs with a mean diameter of 15nm were successfully synthesized via the reduction by borohydride. With CTAB as the capping agent, the nanoparticles were positively-charged and successfully attached to the negatively-charged membrane surface via electrostatic interaction. Additionally, the attachment of CuNPs was accomplished by covalent bonding with thiol group as a bridging group.

The membranes with incorporated Cu-NPs via these two bonding methods were evaluated and compared. Scanning electron microscopy (SEM) imaging and associated energy-dispersive X-ray spectroscopy (EDS) showed that large amounts of Cu-NPs existed on both types of membranes. The hydrophilicity of the membrane surface was all enhanced by the membrane surface modifications. Water flux of the membranes was increased with slight decrease in salt rejection. TFC-S-CuNPs had higher performance in water permeability with the salt rejection remained at 92.26%.

Both Cu-NPs immobilized membranes showed significant anti-bacterial properties against *P. aeruginosa*. TFC-S-CuNPs was observed to be more effective due to its ability to inhibit the bacterial growth in the vicinity of the membrane colony. The covalent bonding was more stable than the attachment through the electrostatic attraction based on the bacterial incubation result after dissolution. The study has demonstrated that Cu-NPs have the potential to be used to modify membranes with antibacterial characteristics.

## **4.2 Future studies**

The priority of the future work is to conduct the dissolution test of TFC-Cu and TFC-S-Cu membranes. The amount of copper ions released by Cu-NPs should be quantified. Monitoring the release of copper ions will allow comparison of two membranes where CuNPs were attached in different ways.

When compared to silver, copper is more easily oxidized. The effect of copper oxide on the membrane surface should be considered and analyzed. The longevity of membranes' antibacterial effect should be assessed. Moreover, approaches to reload CuNPs onto the membrane surface should be explored.

The recent research reported that the shape and size of nanoparticles could be controlled by adjusting the concentration of reducing agent and reaction temperature. It would be interesting to determine the performances of the membranes with different kinds of Cu-NPs.

Nanoparticles synthesized using other metals or new methods could also be explored. If possible, to combine two or more components in the nanostructure to get the alloy-nanoparticles may be of interest.

## BIBLIOGRAPHY

- Akar, N., B. Asar, N. Dizge and I. Koyuncu (2013). "Investigation of characterization and biofouling properties of PES membrane containing selenium and copper nanoparticles." Journal of Membrane Science **437**: 216-226.
- Basri, H., A. F. Ismail, M. Aziz, K. Nagai, T. Matsuura, M. S. Abdullah and B. C. Ng (2010). "Silver-filled polyethersulfone membranes for antibacterial applications - effect of PVP and TAP addition on silver dispersion." Desalination **261**(3): 264-271.
- Beerlage, M. A. M. (1994). "Polyimide ultrafiltration membranes for non-aqueous systems."
- Benavente, E., H. Lozano and G. González (2013). "Fabrication of copper nanoparticles: Advances in synthesis, morphology control, and chemical stability." Recent Patents on Nanotechnology **7**(2): 108-132.
- Cadotte, J. E., R. J. Petersen, R. E. Larson and E. E. Erickson (1980). "A new thin-film composite seawater reverse osmosis membrane." Desalination **32**(C): 25-31.
- Camassola, M., L. M. G. de Macedo Braga, P. C. Chagastelles and N. B. Nardi (2012). Methodology, biology and clinical applications of human mesenchymal stem cells. Somatic Stem Cells: Methods and Protocols, Springer. **vol. 879**: pp. 491-504.
- Cao, X., M. Tang, F. Liu, Y. Nie and C. Zhao (2010). "Immobilization of silver nanoparticles onto sulfonated polyethersulfone membranes as antibacterial materials." Colloids and Surfaces B: Biointerfaces **81**(2): 555-562.
- Chamakura, K., R. Perez-Ballester, Z. Luo, S. Bashir and J. Liu (2011). "Comparison of bactericidal activities of silver nanoparticles with common chemical disinfectants." Colloids and Surfaces B: Biointerfaces **84**(1): 88-96.
- Chen, Y., Y. Zhang, J. Liu, H. Zhang and K. Wang (2012). "Preparation and antibacterial property of polyethersulfone ultrafiltration hybrid membrane containing halloysite nanotubes loaded with copper ions." Chemical Engineering Journal **210**: 298-308.
- Committee, A. M. T. R. (2005). "Committee Report: Recent advances and research needs in membrane fouling." Journal / American Water Works Association **97**(8): 79-89+14.
- Dang, J., Y. Zhang, Z. Du, H. Zhang and J. Liu (2012). "Antibacterial properties of PES/CuCl<sub>2</sub> three-bore hollow fiber UF membrane." Water Science and Technology **66**(4): 799-803.

- Daniel, M. C. and D. Astruc (2004). "Gold Nanoparticles: Assembly, Supramolecular Chemistry, Quantum-Size-Related Properties, and Applications Toward Biology, Catalysis, and Nanotechnology." Chemical Reviews **104**(1): 293-346.
- Dhas, N. A., C. P. Raj and A. Gedanken (1998). "Synthesis, Characterization, and Properties of Metallic Copper Nanoparticles." Chemistry of Materials **10**(5): 1446-1452.
- Ellis, T. N., S. A. Leiman and M. J. Kuehn (2010). "Naturally produced outer membrane vesicles from *Pseudomonas aeruginosa* elicit a potent innate immune response via combined sensing of both lipopolysaccharide and protein components." Infection and Immunity **78**(9): 3822-3831.
- Fritzmann, C., J. Löwenberg, T. Wintgens and T. Melin (2007). "State-of-the-art of reverse osmosis desalination." Desalination **216**(1-3): 1-76.
- Greenlee, L. F. L., Desmond F. ; Freeman, Benny D. ; Marrot, Benoit ; Moulin, Philippe (2009). "Reverse osmosis desalination: Water sources, technology, and today's challenges." Water Research **43**(9).
- Huang, H. H., F. Q. Yan, Y. M. Kek, C. H. Chew, G. Q. Xu, W. Ji, P. S. Oh and S. H. Tang (1997). "Synthesis, characterization, and nonlinear optical properties of copper nanoparticles." Langmuir **13**(2): 172-175.
- Irie, Y., B. R. Borlee, J. R. O'Connor, P. J. Hill, C. S. Harwood, D. J. Wozniak and M. R. Parsek (2012). "Self-produced exopolysaccharide is a signal that stimulates biofilm formation in *Pseudomonas aeruginosa*." Proceedings of the National Academy of Sciences **109**(50): 20632-20636.
- Isloor, A. M., B. M. Ganesh, S. M. Isloor, A. F. Ismail, H. S. Nagaraj and M. Pattabi (2013). "Studies on copper coated polysulfone/modified poly isobutylene alt-maleic anhydride blend membrane and its antibiofouling property." Desalination **308**: 82-88.
- Jeong, B. H., E. M. V. Hoek, Y. Yan, A. Subramani, X. Huang, G. Hurwitz, A. K. Ghosh and A. Jawor (2007). "Interfacial polymerization of thin film nanocomposites: A new concept for reverse osmosis membranes." Journal of Membrane Science **294**(1-2): 1-7.
- Karkhanechi, H., R. Takagi, Y. Ohmukai and H. Matsuyama (2013). "Enhancing the antibiofouling performance of RO membranes using Cu(OH)<sub>2</sub> as an antibacterial agent." Desalination **325**: 40-47.
- Khanna, P. K., S. Gaikwad, P. V. Adhyapak, N. Singh and R. Marimuthu (2007). "Synthesis and characterization of copper nanoparticles." Materials Letters **61**(25): 4711-4714.

- Kim, S. H., S. Y. Kwak, B. H. Sohn and T. H. Park (2003). "Design of TiO<sub>2</sub> nanoparticle self-assembled aromatic polyamide thin-film-composite (TFC) membrane as an approach to solve biofouling problem." Journal of Membrane Science **211**(1): 157-165.
- Klausen, M., A. Heydorn, P. Ragas, L. Lambertsen, A. Aaes-Jørgensen, S. Molin and T. Tolker-Nielsen (2003). "Biofilm formation by *Pseudomonas aeruginosa* wild type, flagella and type IV pili mutants." Molecular Microbiology **48**(6): 1511-1524.
- Koseoglu-Imer, D. Y., B. Kose, M. Altinbas and I. Koyuncu (2013). "The production of polysulfone (PS) membrane with silver nanoparticles (AgNP): Physical properties, filtration performances, and biofouling resistances of membranes." Journal of Membrane Science **428**: 620-628.
- Kulkarni, A., D. Mukherjee and W. N. Gill (1996). "Flux enhancement by hydrophilization of thin film composite reverse osmosis membranes." Journal of Membrane Science **114**(1): 39-50.
- Lee, H. S., S. J. Im, J. H. Kim, H. J. Kim, J. P. Kim and B. R. Min (2008). "Polyamide thin-film nanofiltration membranes containing TiO<sub>2</sub> nanoparticles." Desalination **219**(1-3): 48-56.
- Lee, K. P., T. C. Arnot and D. Mattia (2011). "A review of reverse osmosis membrane materials for desalination-Development to date and future potential." Journal of Membrane Science **370**(1-2): 1-22.
- Lee, S. Y., H. J. Kim, R. Patel, S. J. Im, J. H. Kim and B. R. Min (2007). "Silver nanoparticles immobilized on thin film composite polyamide membrane: Characterization, nanofiltration, antifouling properties." Polymers for Advanced Technologies **18**(7): 562-568.
- Mott, D., J. Galkowski, L. Wang, J. Luo and C. J. Zhong (2007). "Synthesis of size-controlled and shaped copper nanoparticles." Langmuir **23**(10): 5740-5745.
- Parada, M. A., A. de Almeida, P. N. Volpe, C. Muntele and D. Ila (2007). "Damage effects of 1 MeV proton bombardment in PVDC polymeric film." Surface and Coatings Technology **201**(19-20 SPEC. ISS.): 8052-8054.
- Park, B. K., S. Jeong, D. Kim, J. Moon, S. Lim and J. S. Kim (2007). "Synthesis and size control of monodisperse copper nanoparticles by polyol method." Journal of Colloid and Interface Science **311**(2): 417-424.
- Prabhawathi, V., P. M. Sivakumar and M. Doble (2012). "Green synthesis of protein stabilized silver nanoparticles using *Pseudomonas fluorescens*, a marine bacterium, and

its biomedical applications when coated on polycaprolactam." Industrial and Engineering Chemistry Research **51**(14): 5230-5239.

Qiu, J. H., Y. W. Zhang, Y. T. Zhang, H. Q. Zhang and J. D. Liu (2011). "Synthesis and antibacterial activity of copper-immobilized membrane comprising grafted poly(4-vinylpyridine) chains." Journal of Colloid and Interface Science **354**(1): 152-159.

Salzemann, C., I. Lisiecki, J. Urban and M. P. Pileni (2004). "Anisotropic copper nanocrystals synthesized in a supersaturated medium: Nanocrystal growth." Langmuir **20**(26): 11772-11777.

Sawada, I., R. Fachrul, T. Ito, Y. Ohmukai, T. Maruyama and H. Matsuyama (2012). "Development of a hydrophilic polymer membrane containing silver nanoparticles with both organic antifouling and antibacterial properties." Journal of Membrane Science **387-388**(1): 1-6.

Shu, J. Y., K. Majamaa, S. Coker and T. Knoell (2014). Advancing reverse osmosis membrane performance in a water reuse application - A collaborative approach. AWWA/AMTA 2014 Membrane Technology Conference and Exposition.

Tarboush, B. J. A., D. Rana, T. Matsuura, H. A. Arafat and R. M. Narbaitz (2008). "Preparation of thin-film-composite polyamide membranes for desalination using novel hydrophilic surface modifying macromolecules." Journal of Membrane Science **325**(1): 166-175.

Tipton, K. A., J. P. Coleman and E. C. Pesci (2013). "QapR (PA5506) Represses an operon that negatively affects the *Pseudomonas* quinolone signal in *Pseudomonas aeruginosa*." Journal of Bacteriology **195**(15): 3433-3441.

Wharton, C. W. (1986). "Review article: Infra-red and Raman spectroscopic studies of enzyme structure and function." Biochemical Journal **233**(1): 25-36.

Wu, S. H. and D. H. Chen (2004). "Synthesis of high-concentration Cu nanoparticles in aqueous CTAB solutions." Journal of Colloid and Interface Science **273**(1): 165-169.

Xu, J., X. Feng, P. Chen and C. Gao (2012). "Development of an antibacterial copper (II)-chelated polyacrylonitrile ultrafiltration membrane." Journal of Membrane Science **413-414**: 62-69.

Yin, J., E. S. Kim, J. Yang and B. Deng (2012). "Fabrication of a novel thin-film nanocomposite (TFN) membrane containing MCM-41 silica nanoparticles (NPs) for water purification." Journal of Membrane Science **423-424**: 238-246.

Yin, J., Y. Yang, Z. Hu and B. Deng (2013). "Attachment of silver nanoparticles (AgNPs) onto thin-film composite (TFC) membranes through covalent bonding to reduce membrane biofouling." Journal of Membrane Science **441**: 73-82.

Zhang, Y. and Z. Hu (2013). "Combined treatment of *Pseudomonas aeruginosa* biofilms with bacteriophages and chlorine." Biotechnology and Bioengineering **110**(1): 286-295.

Zhu, L. J., L. P. Zhu, Z. Yi, J. H. Jiang, B. K. Zhu and Y. Y. Xu (2013). "Hemocompatible and antibacterial porous membranes with heparinized copper hydroxide nanofibers as separation layer." Colloids and Surfaces B: Biointerfaces **110**: 36-44.

Zhu, X., R. Bai, K. H. Wee, C. Liu and S. L. Tang (2010). "Membrane surfaces immobilized with ionic or reduced silver and their anti-biofouling performances." Journal of Membrane Science **363**(1-2): 278-286.

Zodrow, K., L. Brunet, S. Mahendra, D. Li, A. Zhang, Q. Li and P. J. J. Alvarez (2009). "Polysulfone ultrafiltration membranes impregnated with silver nanoparticles show improved biofouling resistance and virus removal." Water Research **43**(3): 715-723.